

ARTICLE

Freshwater Ecology

Rehydration of degraded wetlands: Understanding drivers of vegetation community trajectories

Andrea Nocentini^{1,2}  | Jed Redwine^{1,3}  | Evelyn Gaiser^{2,4}  | Troy Hill¹  |
 Sophia Hoffman^{2,4}  | John S. Kominoski^{2,4}  | Jay Sah²  | Dilip Shinde⁵ |
 Donatto Surratt⁶

¹South Florida Natural Resource Center, National Park Service, Homestead, Florida, USA

²Institute of Environment, Florida International University, Miami, Florida, USA

³Environmental Resource Management Department, Seminole Tribe of Florida, Clewiston, Florida, USA

⁴Department of Biological Sciences, Florida International University, Miami, Florida, USA

⁵Everglades and Dry Tortugas National Parks, Homestead, Florida, USA

⁶Loxahatchee National Wildlife Refuge, National Park Service, Boynton Beach, Florida, USA

Correspondence

John S. Kominoski

Email: jkominos@fiu.edu

Present address

Andrea Nocentini, Environmental Resource Management Department, Seminole Tribe of Florida, Clewiston, Florida, USA.

Funding information

National Science Foundation,
Grant/Award Numbers: DBI-0620409,
DEB-1237517, DEB-9910514; Everglades National Park, Grant/Award Numbers: H5297-05-0099, P11A50510, P14AC01639, P16AC00032, P16AC01704; Institute of Environment at Florida International University, Grant/Award Number: 1677

Handling Editor: Natalie A. Griffiths

Abstract

Degradation of wetland ecosystems results from loss of hydrologic connectivity, nutrient enrichment, and altered fire regimes, among other factors. It is uncertain how drivers of wetland ecosystem processes and wetland vegetation communities interact in reversing the ecological trajectory from degraded to restored conditions. We analyzed biogeochemical and vegetation data collected in wetlands of the Florida Everglades at the start of (2015) and during (2018 and 2021) the initial stages of rehydration. Our objectives were to analyze the allocation of carbon and nutrients among ecosystem compartments and correlated trajectories of vegetation community change following rehydration, to identify the drivers of change, including fire, and analyze macrophyte species-specific responses to drivers. We expected to see changes in vegetation toward more hydric communities that would differ based on wetland baseline conditions and the magnitude of the hydrologic change. During the study period, both length of inundation and surface water depth increased throughout wetlands in the region, and four fires occurred, which affected 51% of the sampling locations. We observed biogeochemical shifts in the wetland landscape, driven by both hydrology and fire. Total phosphorus concentrations in soil and flocculent detrital material decreased, while soil carbon:phosphorus and nitrogen:phosphorus mass ratios increased at sites further away from water management infrastructure. Transitions in vegetation communities were driven by an increase in hydroperiods and by the distinct changes in nutrient concentrations or soil stoichiometric ratios in each subregion. The abundance

This is an open access article under the terms of the [Creative Commons Attribution License](#), which permits use, distribution and reproduction in any medium, provided the original work is properly cited.

© 2024 The Authors. *Ecosphere* published by Wiley Periodicals LLC on behalf of The Ecological Society of America.

of macrophyte species typical of short-hydroperiod prairies strongly decreased, while dominant long-hydroperiod species, such as *Eleocharis cellulosa*, expanded. Fire facilitated the expansion of thickly vegetated plumes of invasive *Typha* at sites close to the water inflow sources. Overall, restored hydrology shifted vegetation community composition toward higher abundance of long-hydroperiod species within six years. In contrast, removal of invasive vegetation controlled by soil phosphorus concentrations will likely require long-term and interactive restoration strategies.

KEY WORDS

fire, hydroperiod, nonmetric multidimensional scaling, phosphorus, stoichiometry, vegetation community transitions, vegetation recovery, wetland restoration

INTRODUCTION

Agents of transformation, such as land use and climate change, have greatly impacted wetland hydrologic and biogeochemical cycles, causing extensive degradation of these ecosystems (Hu et al., 2020; Li et al., 2018; Zedler & Kercher, 2005) through loss of hydrologic connectivity (Meng et al., 2020), nutrient enrichment (Bricker et al., 2008; Davis & Ogden, 1994; Hagerthey et al., 2008), and altered disturbance regimes, such as fire (Slocum et al., 2007; Williams-Jara et al., 2022). Understanding the alternative controls of community structure and ecosystem function in degraded ecosystems is essential for predicting responses to restoration (Hobbs et al., 2006; Seastedt et al., 2008; Suding et al., 2004). In this context, recognizing and quantifying disturbance legacies provide landscape managers the opportunity to influence the persistence of degraded ecosystem conditions, which is explained by “fast” responses in “slow” variables (Hagerthey et al., 2008; Newman et al., 2017; Scheffer & Carpenter, 2003). Landscapes are an aggregated patchwork of sites with unique disturbance legacies. This phenomenon may be especially prevalent in fragmented ecosystems that are disconnected spatially and temporally, such as many wetland ecosystems, whose mosaic structure originates from patterned morphology, gradients in soil types, and variable hydrology (Cole et al., 1997; Osborne et al., 2011; Van der Valk & Warner, 2008).

Changes in “slow” (i.e., variations occurring over decades) variables of wetlands, such as soil physical properties and nutrient concentrations, are expressed through change in vegetation communities and can even cause regime shifts (Hagerthey et al., 2008; Newman et al., 2017). Regime shifts characterize severely degraded ecosystem conditions, are usually resistant to reversal, and can persist for decades even while restoration actions are installed, due to the difficulty in manipulating slow

variables when strong feedback loops establish between them and distinct ecosystem compartments (Newman et al., 2017; Scheffer & Carpenter, 2003).

Projects to restore wetland ecosystems commonly intervene to reestablish hydrologic regimes (Davis & Ogden, 1994; Sklar et al., 2005; Zedler, 2000). By reestablishing more natural hydrologic conditions, restoration managers may aspire to reshape topography indirectly, by enhancing accretion of organic soils while maintaining stable soil stoichiometric ratios, leading to recovery of native vegetation and faunal diversity and abundance (Yu et al., 2017; Zhao et al., 2016). Nevertheless, restoring hydrologic conditions might not be enough to trigger changes that would help reverse trajectories of the most severely degraded wetlands, where feedback loops have established. Therefore, active management strategies may be adopted to perturb the system and produce the ecological changes that would support vegetation community transitions and the feedbacks necessary to restore more natural biogeochemical characteristics (Newman et al., 2017).

Prescribed fire is an active management strategy that can be used to control excessive aboveground biomass growth, the expansion of invasive species, or to mobilize and recycle nutrients (Nocentini, Kominoski, Sah, Redwine, et al., 2021). Fire is an important controlling variable that causes both short-term and long-term effects on ecosystem stocks and processes (Hurteau & Brooks, 2011; Ojima et al., 1994). In wetland ecosystems, fire interacts with hydrology to drive postfire biogeochemical cycling (Kominoski et al., 2022; Nocentini, Kominoski, & Sah, 2021; Osborne et al., 2013) and vegetation recovery (Kominoski et al., 2022; Ruiz et al., 2013; Sah et al., 2011).

Since 2000, the Comprehensive Everglades Restoration Plan (CERP) has been actively restoring the Florida Everglades (LoSchiavo et al., 2013; National Research Council, 2018). The CERP goals are to restore pre-drainage hydrologic patterns and flow-ways, reestablish the historic

slough, ridge, and tree island landscape mosaic, increase the accretion of organic peat soils, maintain sufficient water quality (i.e., surface water total phosphorus [TP] $<10 \mu\text{g L}^{-1}$), regenerate ecological connectivity and biodiversity, and restore natural fire regimes (McVoy et al., 2011; National Research Council, 2018). The Everglades is an oligotrophic system that assimilates phosphorus (P) through consequent state changes that initially occur in the microbial community and can extend into macrophytes (Gaiser et al., 2005; Hagerthey et al., 2008; Newman et al., 2017). Historically, the Everglades was characterized by long hydroperiods (i.e., total number of days in a year with soil inundated) and sheet flow (i.e., flow of water over the ground surface as a thin, even layer, not concentrated in a channel) of freshwater southward (McVoy et al., 2011). In the past century, large portions of the Everglades were drained for agricultural production and urbanization, as hydrologic connectivity was reduced by the creation of basins via drainage canals, causing extensive ecosystem degradation (Light & Dineen, 1994; National Research Council, 2018). At the same time, agriculture runoff caused serious eutrophication problems through P loading. This excess P loading has resulted in many areas near water inflow points and adjacent to canals being affected by P

enrichment and characterized by substantially higher macrophyte biomass, disappearance of native periphyton mats, and encroachment of invasive species (Gaiser et al., 2005; Noe & Childers, 2007; Sklar et al., 2005).

In the Everglades, herbaceous vegetation is mainly arranged along the hydrologic gradient, which has historically been dictated by morphologic variations in the landscape. Vegetation communities typical of the Everglades wetlands include, arranged along the hydrologic gradient from drier to wetter: muhly grass [*Muhlenbergia capillaris* (Lam.) Trin. Var. *filipes* (M. A. Curtis) Chapm. ex Beal]-dominated prairies, Tracyi's beaksedge (*Rhynchospora tracyi* Britton)-dominated marshes, sawgrass (*Cladium jamaicense* Crantz)-dominated marshes, spikerush (*Eleocharis cellulosa* Torr.)-dominated marshes, and American white waterlily (*Nymphaea odorata* Aiton)-dominated sloughs (Figure 1A–E). Wetland vegetation was found to respond to hydrologic changes with a time lag up to four years (Armentano et al., 2006; Zweig & Kitchens, 2008). For example, within the four-year time frame, *C. jamaicense* replaced *M. capillaris*, and *E. cellulosa* was observed to increase its abundance, to the detriment of *C. jamaicense*, following increases in water depth and extension of hydroperiods (Armentano et al., 2006; Childers et al., 2006), while impoundment

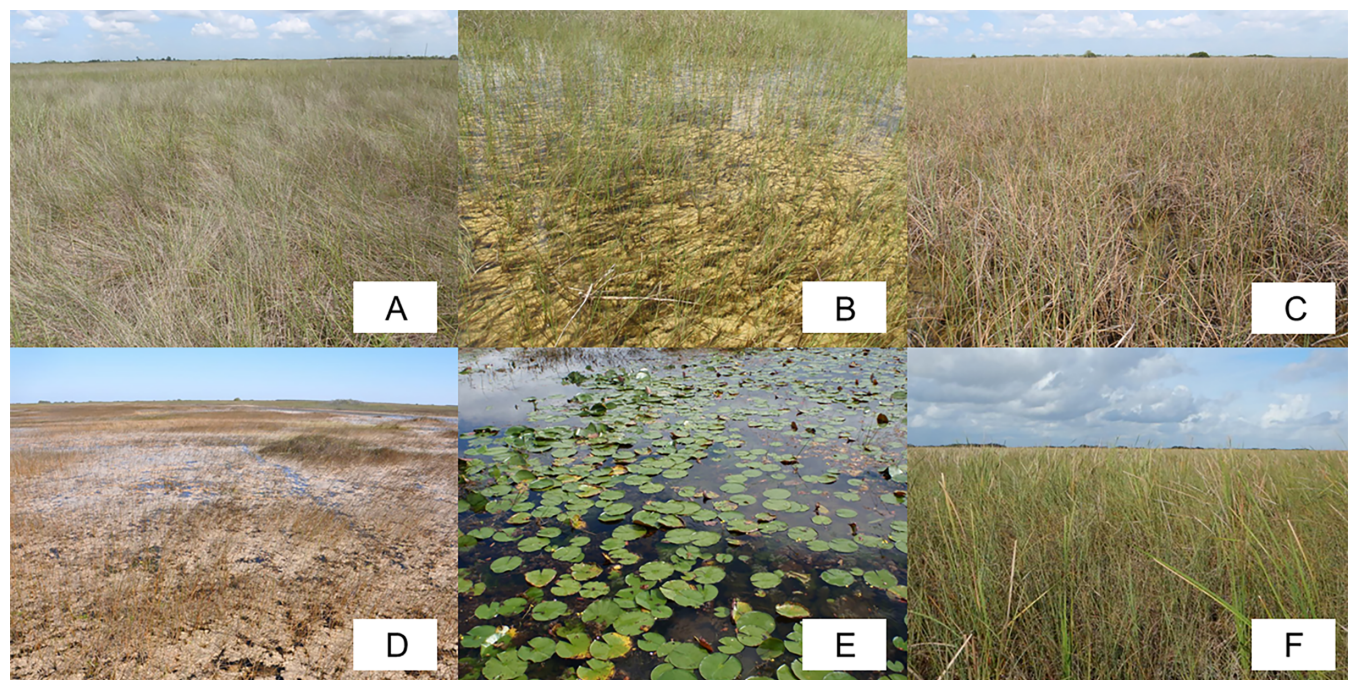


FIGURE 1 Vegetation communities along the hydrologic gradient of Everglades wetlands that can be found in Northeast Shark River Slough (NESRS). From drier to wetter conditions: *Muhlenbergia capillaris* prairie (A), *Rhynchospora tracyi* marsh (B), *Cladium jamaicense* marsh (C), *Eleocharis cellulosa* marsh (D), *Nymphaea odorata* slough (E). Biogeochemistry is another important driver of vegetation community composition (Hagerthey et al., 2008) and, in the Everglades, eutrophication has caused the expansion of invasive *Typha*. In NESRS, the *C. jamaicense*–*Typha* marsh (F), characterized by high aboveground biomass and tall, dense canopies, has developed near water management infrastructures as a result of phosphorus (P) enrichment. Photo credits: South Florida Caribbean Network, U.S. National Park Service.

and continuous inundation brought an expansion of *N. odorata* (Zweig & Kitchens, 2008).

Macrophyte biomass and species composition are also driven by nutrient concentrations in the soil and other ecosystem compartments (Chiang et al., 2000; Craft et al., 1995; Hagerhey et al., 2008; Richards & Ivey, 2004; Sah et al., 2014). Eutrophication of the Everglades has resulted in the expansion of cattail (*Typha* spp.; Surratt et al., 2012) and other invasive species, such as coastal plain willow (*Salix caroliniana* Michx.). Through much of the degraded Everglades wetlands, *Typha* is found in association with tall *C. jamaicense*, forming *C. jamaicense*–*Typha*-dominated marshes (Figure 1F). In contrast, in the northern Everglades, the response to drastic levels of eutrophication has resulted in *Typha*-dominated marshes (Hagerhey et al., 2008; Newman et al., 1996, 1998).

Fire is another factor determining vegetation community transitions in the Everglades (Lockwood et al., 2003), and its occurrence can also be linked to the presence of specific plant species. For example, fire can promote the expansion of *E. cellulosa* and *S. caroliniana* into *C. jamaicense* marshes and bayhead tree communities, respectively (Gunderson, 1994), or it can support the expansion of *Typha* in altered, eutrophic wetlands (Wu et al., 2012). In southern Everglades marshes, lanceleaf arrowhead (*Sagittaria lancifolia* L.) abundance was observed to increase shortly after fire (Nocentini et al., 2022).

Rehydration of Everglades National Park (ENP) was planned within CERP and began in October 2015. The majority of increased water flows are delivered to Northeast Shark River Slough (NESRS), a 350-km² region of ENP where the data for this study were collected. Our

objectives were to (1) analyze changes in carbon and nutrient allocation and concentrations in surface water, soil, and periphyton, and (2) trajectories of vegetation communities in wetlands following landscape-scale rehydration, and (3) determine relationships between macrophyte species-specific changes and hydrology, fire, and biogeochemistry. We predicted that increasing water depth and extended hydroperiods would result in vegetation shifts in the first six years of restored water flows. We anticipated that shifts would be characterized by a reduction in species typical of short-hydroperiod prairies and a corresponding expansion of species that tolerate long hydroperiods or deeper surface water. We anticipated that hydrology- and fire-driven increases in soil P concentrations could promote the expansion of high P-dependent invasive species such as *Typha* (Chiang et al., 2000; Hagerhey et al., 2008; Newman et al., 1998; Surratt et al., 2012). Given the variability in hydrologic and chemical conditions across the vegetated landscape patches within the NESRS region (Sarker et al., 2020), we also expected that the dataset would allow us to identify species-specific responses to the drivers governing wetland ecological trajectories that translate into vegetation community transitions.

METHODS

Study area and monitoring design

NESRS (Figures 2 and 3) is mostly characterized by long hydroperiods and peat soils. However, NESRS was much wetter and had a larger proportion of more hydric plant

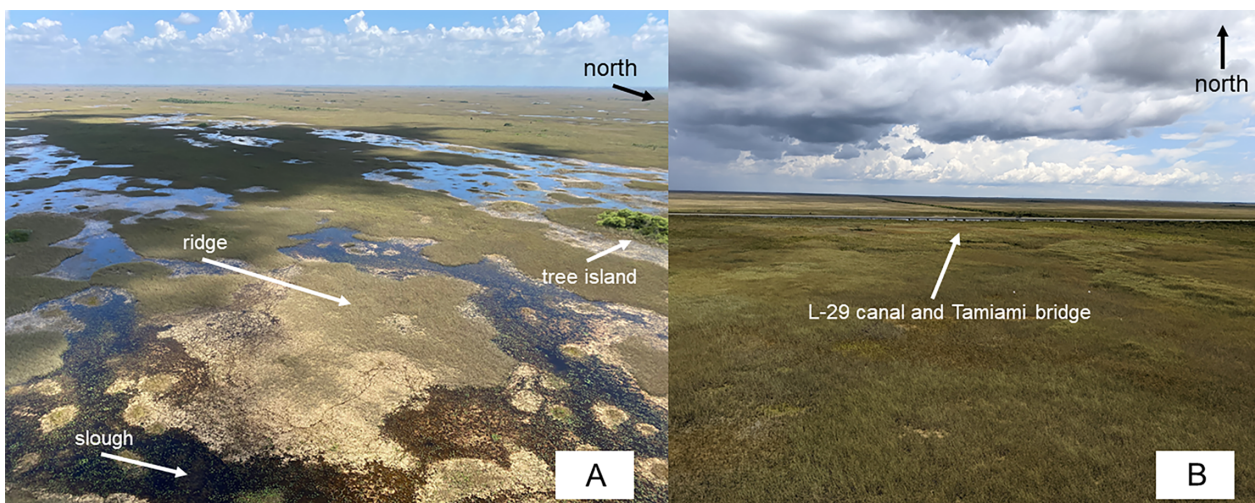


FIGURE 2 Presently, within Northeast Shark River Slough (NESRS), the morphological gradient slough–ridge–tree island, historically characteristic of the Everglades, is recognizable (A), although at different stages of degradation due to drying and eutrophication occurred in the past century. The bridges on Tamiami Trail (B), constructed between 2012 and 2018, are part of the infrastructures that are allowing rehydration of NESRS, as part of Everglades wetlands restoration. Photo credits: Sophia Hoffman (A) and Dylan Scott (B).

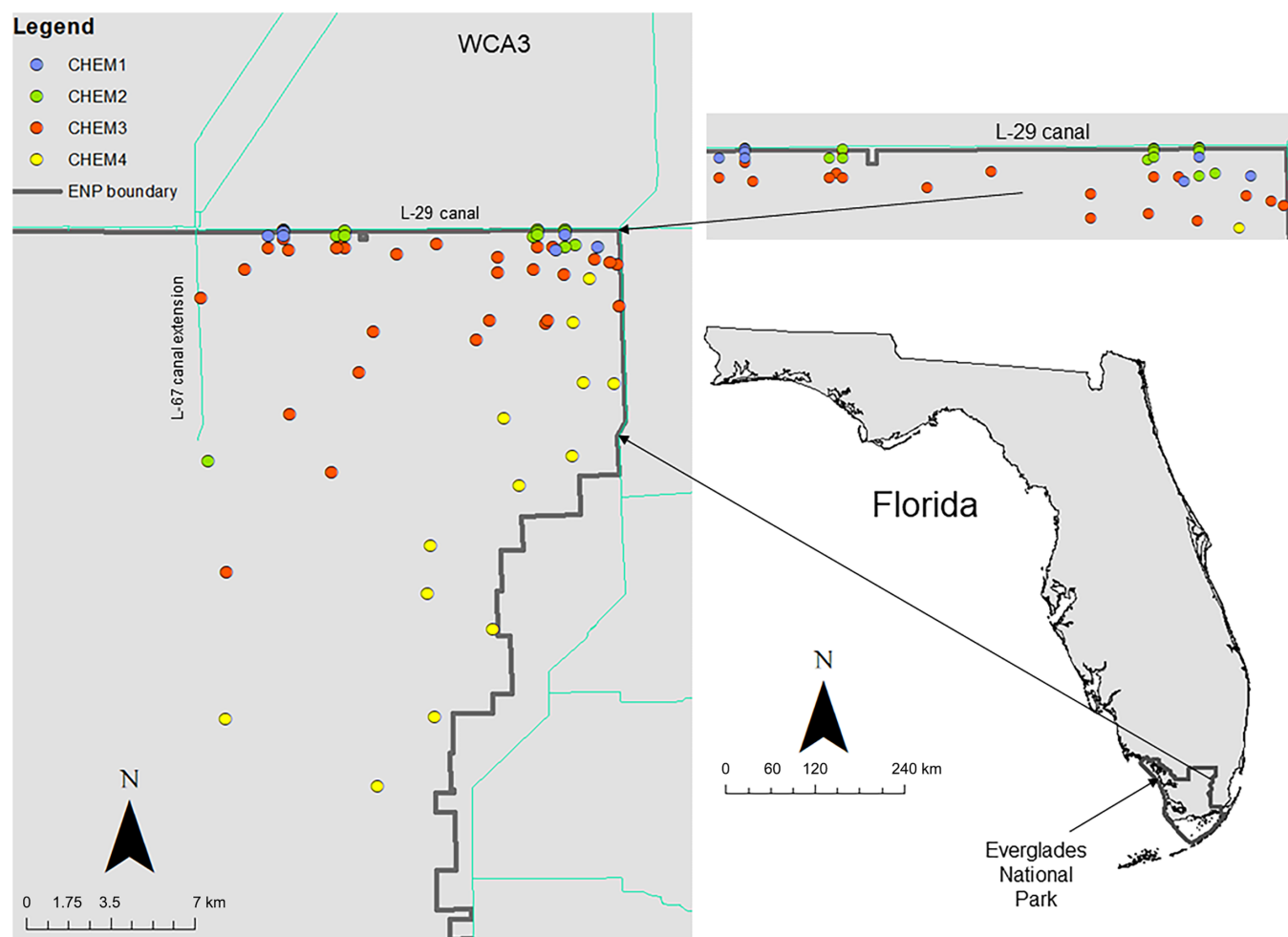


FIGURE 3 Map of the northeast corner of Everglades National Park (ENP). The 65 sites sampled in 2015, 2018, and 2021 are represented by the colored circles. Sites are clustered based on similar biogeochemistry in terms of total carbon, total nitrogen, and total phosphorus concentrations in the periphyton, flocculent detrital material (floc), and soil (for more details, see [Site clustering](#)).

communities (e.g., *E. cellulosa*-dominated marshes and *N. odorata*-dominated sloughs) in the past. Degradation of Shark River Slough began in the late 19th century, became substantial in the 1920s with the construction of the Tamiami Trail road, and intensified in the 1970s with the installation of the L67 A and C levees and canal couplet, which demarcated the boundary of Water Conservation Area (WCA) 3B (McVoy et al., 2011). Compartmentalization through and associated operations of water management infrastructure dried the landscape and led to a partial degradation of the slough–ridge–tree island morphology that was historically characteristic of the region (Figure 2A), and to a substantial expansion of *C. jamaicense* (Sklar et al., 2008). In particular, the loss of hydrologic connectivity significantly reduced the length of inundation in a portion of the southeastern areas of NESRS, causing loss of peat and a shift from historic marshes to prairies in this portion of the Everglades wetland landscape (McVoy et al., 2011).

The NESRS region receives water inflows from the northern WCAs through the L-29 canal (referred to just as canal hereafter). The canal and levees on either side reduce hydrologic connectivity between the northern WCAs and NESRS, constraining water flow to NESRS only via L-29 water control structures S-333 and S-356, and subsequent culverts beneath the Tamiami Trail road. Hydrologic restoration of the region was initiated in 2012 with the construction of a 1.6-km bridge and removal of the roadbed, which enabled overland flow when canal stages are above 2.3 m (National Geodetic Vertical Datum 1929 [NGVD29]). The S-356 pump station was constructed in 2015, allowing seepage to return into NESRS. Two additional bridges (totaling 4.2 km) were completed in 2018 (Figure 2B), further reestablishing hydrologic connectivity, and increasing water deliveries southward. Rehydration of NESRS began in October 2015 with an increase in the maximum stage in the L-29 canal from 2.2 to 2.6 m NGVD29. In September 2020, the Combined Operational Plan (U.S Army Corps of

Engineers, 2023) was adopted, prescribing even higher water flows to NESRS.

Sarker et al. (2020) observed a mean 87-day increase in hydroperiod in NESRS between 2015 and 2018. They also found that P concentrations in the distinct ecosystem matrices (i.e., soil, periphyton, and macrophytes) of NESRS wetlands are characterized by a patchy distribution and declined logarithmically with downstream distance from the canal. Between 2015 and 2018, they observed an increase in periphyton and macrophyte P concentrations only at sites within 1 km from the L-29 canal, reflecting legacy P loading (Sarker et al., 2020). Risks associated with nutrient loading in the context of rehydration are regulated by the consent decree, which has a long-term flow-weighted TP concentration target of $8 \mu\text{g L}^{-1}$ for waters released into Shark River Slough (United States v. SFWMD, et al., Defendants, 1988); when this target is achieved, it results in some control over nutrient loading in the region.

C. jamaicense is the ubiquitous plant species of the NESRS region (similar to the majority of the Everglades landscape; Foti et al., 2012). Compared with the rest of NESRS, *C. jamaicense* density and biomass are substantially greater in proximity of the canal, where it is found together with two other species commonly observed in chronically disturbed Everglades environments: *Typha* and *S. caroliniana*. The presence of thick vegetation plumes, characterized by tall *C. jamaicense* communities with *Typha* and *S. caroliniana*, is due to P enrichment and chronic hydrologic disturbance that occurs frequently around water inflow points (Surratt et al., 2012).

Periphyton is another common feature of NESRS. This association of algae, bacteria, fungi, and microfauna can form thick mats, which cover limestone sediments, coat the submerged stems of macrophytes, or develop into rafts floating in the water. A substantial presence of periphyton is usually observed in areas where macrophyte biomass is sparse and light penetrates the water column without significant obstruction (Gaiser et al., 2011).

The NESRS region has been monitored by ENP since 2006. The soil, periphyton, and plant species responses to water inflows before and after rehydration are monitored along a set of eight transects, complemented by a set of sampling sites distributed across the full area of the wetland. Each of eight transects starts near the canal, runs southward, and consists of five to seven sites ($n = 48$ total transect sites). The other group of sampling sites (i.e., census sites) is randomly distributed throughout the region ($n = 40$ total census sites) and was established to study the restoration effects at a larger spatial scale. The transect sites have been sampled twice every year, in the dry and wet seasons (dry season sampling: March–April; wet season sampling: September–November),

since 2015, whereas the census sites, visited once a year in the wet season, were sampled in 2006, 2007, and 2008, and then every three years starting in 2012. In the present study, we are comparing results from the sampling that occurred in 2015, 2018, and 2021, as these were the only years where all the sites, transect and census, were sampled contemporaneously. Some sites were moved or removed between 2015 and 2018 due to bridge construction, and therefore excluded from the analysis. The northernmost site of each transect was a canal site with no vegetation where only surface water chemistry was measured, and therefore these were only used to investigate the quality of the water delivered to NESRS between 2015 and 2021. The total number of sites used for our analysis was $n = 65$.

Field data collection

Data were collected in November 2015, October 2018, and October 2021. Three 1-m² plots were sampled at each site during each sampling event. We collected surface water, periphyton, soil, and flocculent detrital material (floc hereafter; defined as the “unconsolidated” layer lacking coherence on top of the soil; Larsen et al., 2009). Detailed methods used for sample collection of water, periphyton, soil, and floc are reported in Sarker et al. (2020) and Hoffman, Rizzie, Nocentini, Sarker, et al. (2021). Briefly, 500 mL of unfiltered surface water was collected in plastic bottles, periphyton was collected as a grab sample of 120 mL and stored in sealed plastic bags, while soil and the overlaying floc were sampled by intact coring down to 10-cm soil depth and stored in plastic bags and tubes. The samples were stored on ice until returned to the laboratory. All the abovementioned samples were analyzed for total organic carbon (TOC, surface water) or total carbon (TC), total nitrogen (TN), and TP concentrations. For water samples, TOC was analyzed using a Shimadzu TOC Analyzer (Shimadzu Corporation, Columbia, USA), TN was analyzed with an Antek TN Analyzer (Antek Instruments, Houston, USA), and TP was analyzed according to Solórzano and Sharp (1980). Oven-dried periphyton, soil, and floc samples were analyzed for TC and TN using a Carlo-Erba NA-1500 CNS Analyzer (CE Elantech, Lakewood, USA), and TP concentrations through dry combustion and hydrolysis of the P-containing compounds in the sample (Solórzano & Sharp, 1980), followed by standard colorimetric analysis. Soil stoichiometric mass ratios were calculated using the collected TC, TN, and TP concentrations. Vegetation height and count of live and dead leaves of each plant species present were recorded at each sample plot (Table 1; Hoffman, Rizzie, Nocentini, Tobias, et al., 2021).

TABLE 1 Scientific, common, abbreviated names, and frequencies of the 18 macrophyte species encountered in the years 2015, 2018, and 2021 at the 65 monitoring sites included in the study.

Scientific name	Common name	Abbreviation	Frequency (%)		
			2015	2018	2021
<i>Cladium jamaicense</i> Crantz	Sawgrass	CLAJAM	83	80	83
<i>Eleocharis cellulosa</i> Torr.	Spikerush	ELECEL	51	52	49
<i>Rhynchospora tracyi</i> Britton	Tracyi's beaksedge	RHYTRA	37	32	5
<i>Panicum hemitomon</i> Schult.	Maidencane	PANHEM	35	31	14
<i>Typha</i> spp.	Cattail	TYPSPP	22	26	31
<i>Justicia angusta</i> (Chapm.) Small	Pineland water-willow	JUSANG	20	2	0
<i>Paspalidium geminatum</i> (Forssk.) Stapf	Egyptian panicgrass	PASGEM	15	14	6
<i>Sagittaria lancifolia</i> L.	Lanceleaf arrowhead	SAGLAN	12	2	2
<i>Pontederia cordata</i> L.	Pickerelweed	PONCOR	11	15	11
<i>Crinum americanum</i> L.	Florida swamplily	CRIAME	11	11	5
<i>Muhlenbergia capillaris</i> (Lam.) Trin. Var. <i>filipes</i> (M. A. Curtis) Chapm. ex Beal	Gulfhairawn muhly	MUHCAP	9	3	2
<i>Leersia hexandra</i> Sw.	Southern cutgrass	LEEHEX	9	2	0
<i>Salix caroliniana</i> Michx.	Coastal plain willow	SALCAR	8	12	5
<i>Hymenocallis latifolia</i> (Mill.) M. Roem.	Perfumed spiderlily	HYMLAT	8	5	5
<i>Panicum tenerum</i> Bey.	Bluejoint panicgrass	PANTEN	8	0	3
<i>Dichanthelium</i> spp. (Hitchc. and Chase) Gould	Rosette grass	DICSPP	6	0	2
<i>Rhynchospora microcarpa</i> Baldw.	Southern beaksedge	RHYMIC	3	3	0
<i>Nymphaea odorata</i> Aiton	American white waterlily	NYMODO	3	2	0

Note: "Frequency" corresponds to the percentage of sites where the plant species were encountered in any of the three separate sampling events.

When woody species (e.g., *S. caroliniana*) were encountered, the number of live and dead individuals was recorded.

Vegetation biomass estimation

An estimate of the relationship between leaf counts and dry biomass of plant species was developed in February 2021. Leaves (or individuals, in the case of *S. caroliniana*) of all the species recorded at least three times in 2015 and 2018 were collected. If a species could not be found at the sites, it was collected nearby. Vegetation height was also measured at the time of each sample collection, as the size and biomass of some species varied within the region. For example, *C. jamaicense* grows very thick and tall (above 2 m) near the canal, but in other areas (e.g., areas with deeper water and lower soil nutrient concentration) its density decreases substantially, as well as its height, down to 0.4 m (Hoffman, Rizzie, Nocentini, Tobias, et al., 2021). Upon returning to the laboratory, leaves were divided into live and dead and counted. The total fresh mass of each sample was weighed, and then a subsample was dried in the oven for dry mass conversion. The resulting

relationships between vegetation height, leaf counts, and dry biomass were defined and applied to sample data in order to convert leaf counts into estimates of biomass (Appendix S1: Table S1).

Hydrology and fire metrics

Daily average surface water stage data were obtained from the Everglades Depth Estimation Network (EDEN) database (U.S. Geological Survey, 2020). Surface water depths for all sites were calculated as the difference between estimated water stages (EDEN) and ground elevation obtained from a digital elevation model (U.S. Geological Survey, 2019), using a script in R version 4.2.1 (R Core Team, 2022). Because of EDEN's spatial resolution of 400 m, water depths were adjusted using specific offset measured directly at each site. Surface water depths ≤ 0 cm were considered dry, and water depths > 0 cm were considered wet. Surface water depths were used to calculate the following hydrology metrics at each site and for each sampling event: hydroperiod, days since dry-down, recent dry-down duration, and water depth. Hydroperiod was calculated as the total number of days

with soil inundated (i.e., EDEN water depth >0 cm) within the water year. In subtropical regions, the water year is used to characterize the wet (May 1–October 31) and dry (November 1–April 30) seasons: water year 2015 (May 2014–April 2015), water year 2018 (May 2017–April 2018), water year 2021 (May 2020–April 2021). Days since dry-down was calculated as the total number of days between the end of the last dry-down and the date when those samples were collected. Recent dry-down duration was calculated as the total number of days with the soil dry in the last dry-down event before sampling. Water depth was calculated as the mean of the 365-day water depths prior to sampling. Long-term mean monthly water depths were calculated across all sampling sites and a polynomial, quadratic function was fitted to the regression to analyze the temporal hydrologic trend of the region between 2007 and 2021.

We used fire history data recorded from 1948 to 2021 by ENP (Smith III et al., 2015; fire data for the most recent years are unpublished and were provided to us by ENP), summarized into GIS maps. The database includes location, fire perimeter, burned area, and date of each fire. Time since last fire (TSLF) was calculated at each site and for each sampling event by overlaying the referenced sampling points on fire maps using ArcMap 10.8.1 (Esri, Redlands, California, USA) and is expressed as the number of years elapsed between the last fire event and the year of sampling.

Data analysis

For all statistical analyses, we used R version 4.2.1 (R Core Team, 2022). The R libraries that we employed for data analysis were “stats,” “rstatix,” “vegan,” and “indicspecies.”

Comparison of the hydrology metrics among sampling years was performed using the nonparametric Friedman test, followed by a Wilcoxon post hoc test for pairwise comparisons.

Biogeochemical data collected at 65 sites in 2015, 2018, and 2021 were summarized, first separately, with a nonmetric multidimensional scaling (NMDS) ordination. The data used to generate the ordination were TC, TN, and TP concentrations in periphyton, floc, and soil. After generating a distinct NMDS ordination for each sampling year, sites were grouped into four distinct clusters using *k*-means clustering, based on the ordination that produced the lowest best solution-stress value.

In order to study time trajectories between sampling events, and the role of abiotic variables in explaining changes over time, biogeochemical data from all sampling years (i.e., 2015, 2018, and 2021) were summarized together, again using NMDS, and hydrologic and fire variables (hydroperiod, days since dry-down, recent

dry-down duration, water depth, TSLF) were fitted into the ordination. A permutational multivariate analysis of variance (PERMANOVA) was conducted on the distance matrix to investigate whether significant shifts in wetland biogeochemistry occurred in time and whether any of the abiotic variables had a significant effect on wetland biogeochemical variability. The hydroperiod and TSLF variables were chosen for this analysis. Performing the PERMANOVA requires the environmental variables to be transformed from continuous to categorical, so sites were grouped by length of hydroperiod (short = 0–210 days, intermediate = 211–299 days, and long ≥ 300 days) and by TSLF (short = 0–1 years, intermediate = 2–5 years, and long > 5 years). A 210-day hydroperiod was identified by long-term research in Everglades wetlands as the threshold between prairie and marsh community habitats (Sah et al., 2016). The “simper” function in R was then applied to decompose the Bray–Curtis dissimilarity index (Clarke, 1993). This procedure was used to determine which biogeochemical pools contributed the most to dissimilarities among years.

Differences in carbon and nutrient concentrations of soil, floc, periphyton, and surface water among years and site clusters were analyzed with a Welch’s one-way ANOVA, followed by a Games–Howell post hoc test for pairwise comparisons. Welch’s ANOVA was chosen when variance was not homogeneous among groups (Levene’s test $p < 0.05$). Welch’s ANOVA was also used to analyze the mean distances from the canal of the sites belonging to each site cluster. We introduced one exception in the calculation of the distance from the canal for one site that, because of its proximity, receives water inflows directly from the L-67 canal extension (Figure 3): for this one site, we used the distance from the L-67 canal extension as distance from the canal.

Vegetation patterns and change over time were investigated by calculating importance values (IVs) that summarize plant species abundance within each site cluster. The IVs are calculated as follows:

$$IV_i = ((RF_i + RD_i + RB_i) \div 3) \times 100, \quad (1)$$

where RF_i is the relative frequency, RD_i is the relative density, and RB_i is the relative biomass for each species in each site cluster. All variables in Equation (1) are expressed in percentages and therefore the IV for a single species could range between 0 and 100. We calculated the IVs for 18 species, which are those species encountered at least three times during the study period. The IVs were calculated separately for the three sampling years.

The vegetation data collected at the 65 sites in 2015, 2018, and 2021 were also summarized together using NMDS. To generate the ordination, we used IVs, this

time calculated for each species at each sampling site only using RDi and relative biomass (RBi):

$$IVi = ((RDi + RBi) \div 2) \times 100. \quad (2)$$

After generating the ordination, PERMANOVA was used on the distance matrix to investigate whether a significant transition of vegetation communities along the ecological trajectory occurred in time, and which abiotic variables were driving the variability in vegetation composition. Hydroperiod, biogeochemistry, and TSLF variables were chosen as ecological drivers of vegetation communities. For hydroperiod and TSLF, sites were grouped as described above, while, for biogeochemistry, the clusters previously identified using NMDS were used. In the next step, we rotated the ordination iteratively so that every time axis 1 resulted parallel to hydrologic, fire, or biogeochemical variables. After each rotation, the axis 1 scores were extracted. The extracted scores were then used as predictors of the IVs of dominant species characterizing the distinct vegetation communities of Everglades wetlands and encountered in the NESRS region; polynomial, quadratic functions were fitted to the species-specific regressions. This last step followed the analytical process used by Sah et al. (2014).

Finally, a multilevel pattern analysis (a type of indicator species analysis; De Cáceres et al., 2016) was

applied to test for significant associations between plant species IVs and sites grouped by hydrology, fire, and soil nutrient characteristics (“multipatt” function in R).

RESULTS

Site clustering

Best solution-stress values for the ordinations generated using biogeochemical data from 2015, 2018, and 2021 corresponded to 0.081, 0.066, and 0.071, respectively. Based on the ordinations stress values, the clusters identified with the 2018 biogeochemistry data were selected to be used in subsequent analyses (i.e., CHEM1, CHEM2, CHEM3, and CHEM4; Figure 4). The clustering process allowed us to identify subregions that likely differed in their history of disturbances, resulting in distinct biogeochemical traits and biological organization of the wetlands that are being restored.

The site clusters differed in their distance from the canal. Mean (\pm SD) distance from the canal was 0.40 ± 0.33 , 0.31 ± 0.31 , 2.86 ± 3.15 , and 12.02 ± 6.76 km for CHEM1, CHEM2, CHEM3, and CHEM4, respectively (Table 2). General soil characteristics, also differentiating the site clusters, are described in Appendix S1: Table S2.

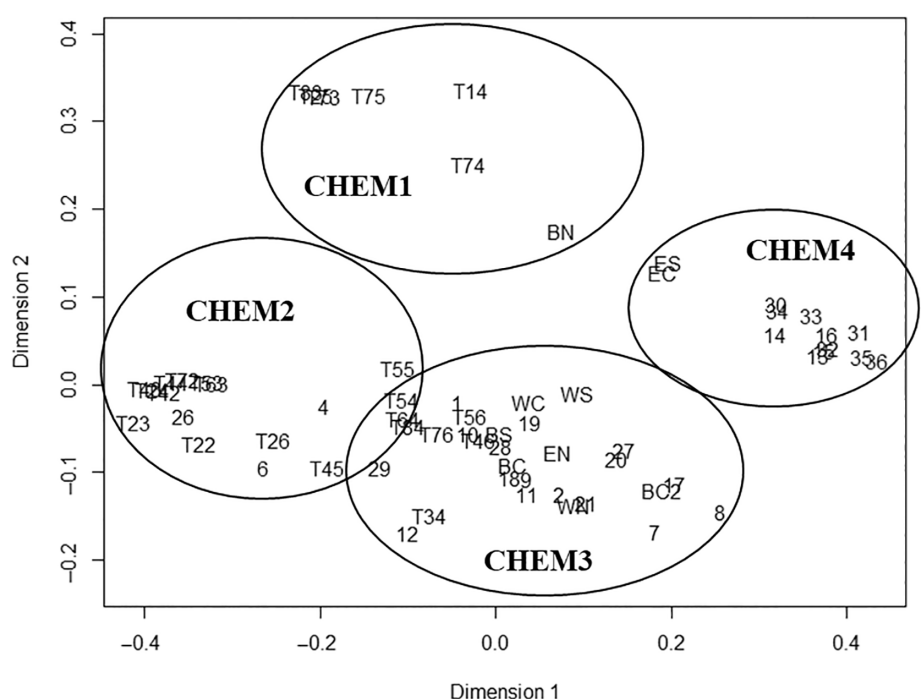


FIGURE 4 Biplot showing the results from the nonmetric multidimensional scaling ordination, based on the biogeochemical characteristics of the 65 sites sampled in the year 2018, namely, total carbon, total nitrogen, and total phosphorus concentrations in periphyton, flocculent detrital material (floc), and soil. Each object in the biplot represents a distinct sampling event (i.e., sampling site \times sampling year) and it is identified by the code representing the sampling site name abbreviation. Four clusters of sites, named CHEM1 ($n = 7$), CHEM2 ($n = 15$), CHEM3 ($n = 30$), and CHEM4 ($n = 13$), were identified using k -means clustering.

Hydrology and fire drivers

Mean hydroperiod and mean water depth were substantially higher in water year 2018 than water year 2015, and substantially higher in water year 2021 than water year 2018 (Table 3). Also, days since dry-down

TABLE 2 Results from Welch's one-way ANOVA, comparing distance from the canal between site clusters (CHEM1, CHEM2, CHEM3, and CHEM4) identified with the nonmetric multidimensional scaling ordination based on biogeochemical traits of periphyton, floc, and soils.

Site cluster	CHEM1	CHEM2	CHEM3
CHEM2	ns
CHEM3	***	***	...
CHEM4	***	***	**

Abbreviation: ns, not significant.

** $p < 0.01$; *** $p < 0.001$.

increased in 2018 compared with 2015, and in 2021 compared with 2018, while recent dry-down duration substantially decreased in 2018 compared with 2015, but did not change much between 2018 and 2021 (Table 3). Statistically significant changes occurred across all site clusters, but the degree of change of hydrologic metrics was greater in some groups. Analysis of monthly mean water depths for the 65 sites in the long term (2007–2021; Figure 5) shows an increase in water depths, during both dry and wet seasons, beginning after the onset of rehydration in October 2015 (Figure 5). The increase in water depths was at least in part attributable to the onset of NESRS rehydration, as it corresponded to a simultaneous increase in water deliveries to the region per unit of rainfall received (Appendix S1: Figure S1).

TSLF greatly varied across the sampling sites, spanning from 1 to over 50 years. Four fires occurred within the NESRS region between the 2015 and 2021 sampling events: the “Airboat” wildfire burned 0.8 km² in the

TABLE 3 Mean (\pm SD) of hydrologic metrics for the three sampling years (2015, 2018, and 2021), summarized by the four site clusters (CHEM1, CHEM2, CHEM3, and CHEM4) identified with the nonmetric multidimensional scaling ordination based on biogeochemical traits of periphyton, floc, and soils.

Hydrology metric	Site cluster	Year 2015	Year 2018	Year 2021	p
Hydroperiod	CHEM1	293 \pm 13	322 \pm 9	343 \pm 1	<0.01
	CHEM2	312 \pm 21	328 \pm 12	345 \pm 3	<0.001
	CHEM3	317 \pm 33	329 \pm 14	346 \pm 4	<0.001
	CHEM4	208 \pm 71	274 \pm 44	338 \pm 9	<0.001
	All sites	292 \pm 58	317 \pm 31	344 \pm 6	<0.001
Days since dry-down	CHEM1	230 \pm 49	397 \pm 155	498 \pm 17	<0.01
	CHEM2	235 \pm 56	501 \pm 217	493 \pm 16	<0.001
	CHEM3	154 \pm 65	419 \pm 202	504 \pm 22	<0.001
	CHEM4	73 \pm 42	167 \pm 131	322 \pm 204	<0.01
	All sites	165 \pm 81	385 \pm 221	465 \pm 117	<0.001
Recent dry-down duration	CHEM1	143 \pm 13	50 \pm 11	55 \pm 7	<0.01
	CHEM2	121 \pm 34	49 \pm 13	44 \pm 11	<0.001
	CHEM3	113 \pm 48	43 \pm 16	44 \pm 24	<0.001
	CHEM4	230 \pm 79	75 \pm 40	67 \pm 32	<0.001
	All sites	141 \pm 68	51 \pm 25	50 \pm 24	<0.001
Water depth (cm)	CHEM1	20 \pm 4	41 \pm 5	55 \pm 6	<0.01
	CHEM2	24 \pm 6	45 \pm 6	58 \pm 6	<0.001
	CHEM3	18 \pm 9	48 \pm 9	60 \pm 9	<0.001
	CHEM4	-11 \pm 18	31 \pm 17	41 \pm 19	<0.001
	All sites	14 \pm 16	43 \pm 12	55 \pm 13	<0.001

Note: Hydroperiod is the total number of days with soil inundated within the water year (May 1–April 30). Days since dry-down is the total number of days elapsed since the last dry-down. Recent dry-down duration is the total number of days with the soil dry in the last dry-down event before sampling. At each site, water depth was calculated as the mean water depth of the 365 days prior to sampling. The p values resulted from the nonparametric Friedman test were used to analyze among-year variation.

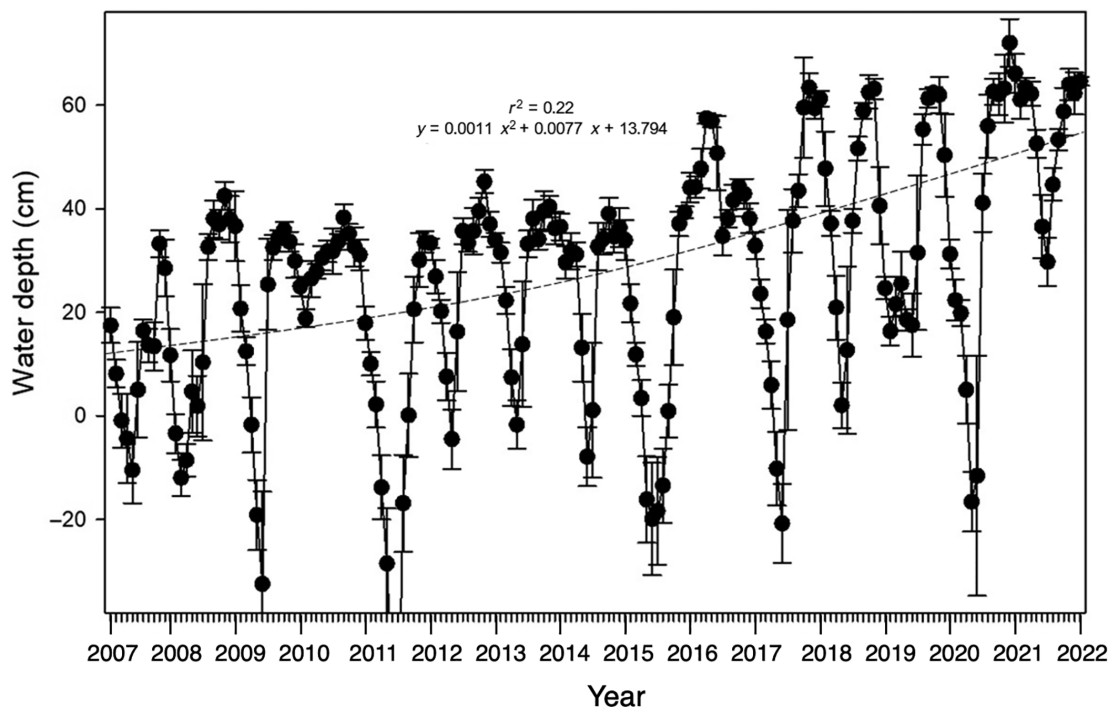


FIGURE 5 Mean monthly water depth calculated for the 65 sites included in the study for the period January 2007 to December 2021. The Figure shows how water depths, in both the dry and wet seasons, increased in Northeast Shark River Slough after the beginning of rehydration in October 2015 compared with the period before rehydration (January 2007–October 2015). Error bars represent the SD from the mean.

TABLE 4 Mean (\pm SD) of time since last fire and percent of sites burned between the 2015 and 2018, and between the 2018 and 2021 sampling events for the 65 sites included in the study, summarized by the four clusters (CHEM1, CHEM2, CHEM3, and CHEM4) identified with the nonmetric multidimensional scaling ordination based on biogeochemical traits of periphyton, floc, and soils.

Site cluster	Time since last fire (years)			Sites burned (%)	
	2015	2018	2021	2015–2018	2018–2021
CHEM1	5.4 \pm 1.6	4.0 \pm 3.7	7.0 \pm 3.7	42.9	0
CHEM2	5.0 \pm 1.0	1.1 \pm 2.3	4.1 \pm 2.3	80.0	0
CHEM3	5.5 \pm 2.0	4.8 \pm 4.2	7.5 \pm 4.5	40.0	3.3
CHEM4	16.3 \pm 16.0	18.4 \pm 16.8	10.6 \pm 8.9	7.7	23.1

north-central portion of NESRS in May 2017, affecting 4 sampling sites, the “EE2” prescribed fire burned 37.0 km² in the northeastern portion of NESRS in March 2018, affecting 25 sampling sites, the “Northeast EE-3 RX” prescribed fire burned 17.6 km² in the central-eastern portion of NESRS in February 2021, affecting 3 sampling sites, and the “Northeast Corner” prescribed fire burned 9.9 km² in the central-western portion of NESRS in June 2021, affecting 1 sampling site. In Table 4, we summarized fire information for each site cluster.

Wetland landscape chemistry

The NMDS ordination on biogeochemical traits of periphyton, floc, and soils allowed us to examine the shifts that occurred between the three sampling events, and the variability among site clusters (Figure 6). Biogeochemistry of all four site clusters shifted in the direction of increasing hydroperiod and decreasing recent dry-down duration. Only the CHEM4 cluster, between 2015 and 2018, shifted in the direction of increasing TSLF, becoming chemically more distinct from the other site clusters (Figure 6).

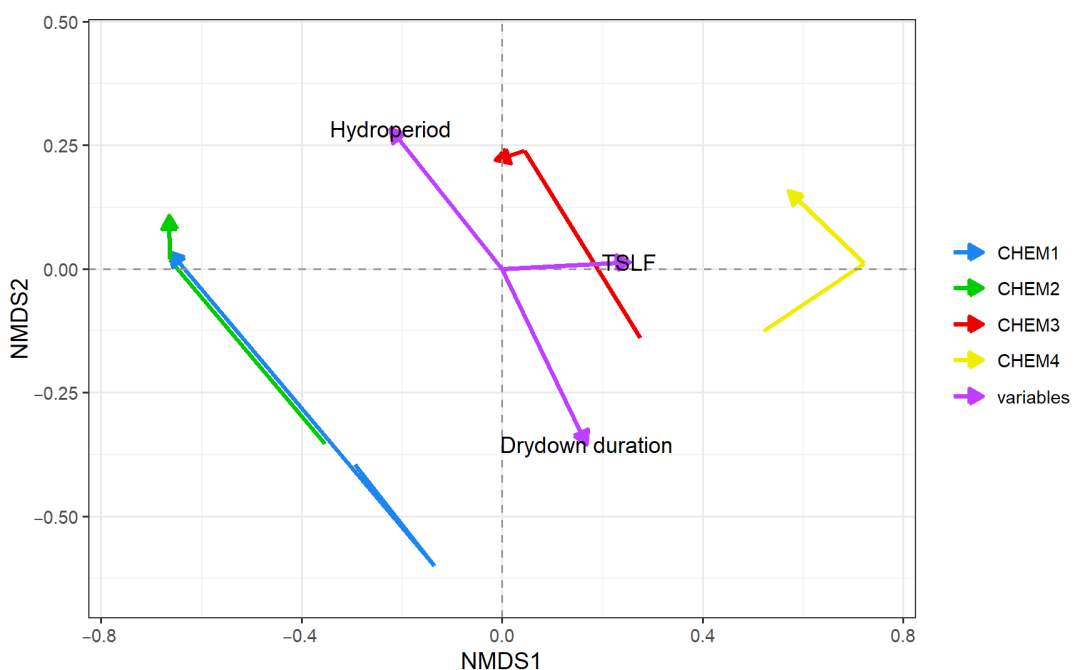


FIGURE 6 Nonmetric multidimensional scaling (NMDS) ordination based on biogeochemical characteristics recorded at the 65 monitoring sites in 2015 (tail of arrows), 2018 (elbow of arrows), and 2021 (tip of arrows). Best solution-stress value corresponded to 0.091. Arrows represent the biogeochemical shift of each site cluster (CHEM1, CHEM2, CHEM3, and CHEM4) between the three sampling years. Site clusters were identified with the NMDS ordination based on biogeochemical traits of periphyton, floc, and soils. Purple arrows represent the direction and load of environmental variables, which were fitted into the ordination. TSLF, time since last fire.

TABLE 5 Results from the permutational multivariate analysis of variance, run on the wetland biogeochemistry distance matrix.

Independent variable	SS	R ²	F	p
Year	1.859	0.100	13.998	0.001
Hydroperiod	2.495	0.135	18.786	0.001
TSLF	0.653	0.035	4.920	0.001
Year × hydroperiod	0.799	0.043	4.013	0.002
Year × TSLF	0.645	0.035	2.428	0.010
Hydroperiod × TSLF	0.143	0.008	2.154	0.097

Note: The analysis was used to test for significant biogeochemical shifts in time and to test hydroperiod (i.e., total number of days in a year with soil inundated) and time since last fire (TSLF) as ecological drivers (independent variables) of wetland biogeochemical variability. The effects of abiotic variable interactions were tested as well. The *p* values reported in boldface denote a statistically significant (<0.05) effect.

The PERMANOVA analysis confirmed that there was a significant shift in time in wetland biogeochemistry, and that hydroperiod and TSLF were both drivers of wetland biogeochemical variability in the NESRS region (Table 5). Also, a significant interaction was found between year and hydroperiod, and between year and TSLF in driving biogeochemical variability (Table 5).

Soil, floc, and periphyton TP concentrations explained 34%–69% of dissimilarities among years within site clusters. Floc TP of CHEM3 decreased by 65% and 54% in 2018 and 2021, respectively, compared with 2015 ($p < 0.001$; Figure 7). Soil TP was consistently higher in CHEM1 and CHEM2 than in CHEM3 and CHEM4 in all sampling years (Figure 7). At the same time, soil TP of CHEM4 was 44% and 39% lower in 2018 and 2021, respectively, than in 2015 ($p < 0.05$). The decrease in soil TP that occurred in CHEM4 caused an increase in soil C:P ratios ($p < 0.01$). Although the decrease in soil TP that occurred in CHEM3 was small and not statistically significant, it caused a significant increase in soil C:P and N:P ratios ($p < 0.05$; Figure 8). Mean periphyton TP concentration in CHEM2 increased between 2018 and 2021 ($p < 0.001$), while it remained low in CHEM3 and CHEM4 throughout the study period (Figure 9). The CHEM3 and CHEM4 clusters registered higher surface water TP concentrations in 2018 compared with 2015 ($p < 0.001$; Figure 9). Mean surface water TP in CHEM3 was also higher in 2021 than in 2015 ($p < 0.05$), while it decreased in CHEM4 in 2021 (Figure 9). At the same time, while seasonal variability of surface water TP concentrations in the canal was high during the study period, mean surface water TP concentrations in the canal did not differ between the three sampling years.

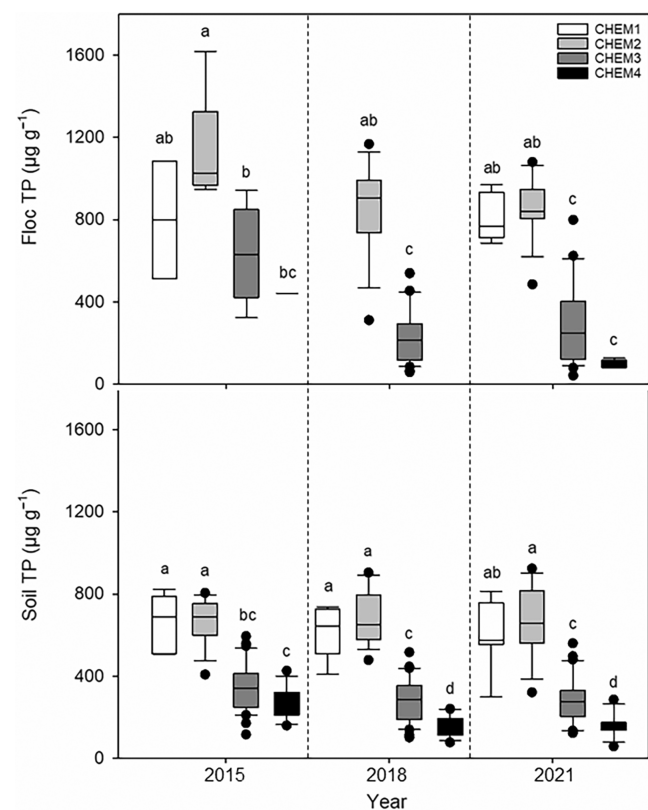


FIGURE 7 Box plot of total phosphorus (TP) concentrations in the flocculent detrital material (floc) and in the soil for the three sampling years (2015, 2018, and 2021), summarized by the four site clusters (CHEM1, CHEM2, CHEM3, and CHEM4) identified with the nonmetric multidimensional scaling ordination based on biogeochemical traits of periphyton, floc, and soils. Letters identify significance groupings among site clusters and years at $p \leq 0.05$, based on the results from Welch's one-way ANOVA. The midline of boxplots represents the median, box limits are the upper and lower quartile values, whiskers are the SE, and points above box plots indicate outliers.

("Wet2015," "Wet2018," and "Wet2021"; Appendix S1; Figure S2).

Vegetation community transitions

Six years after increasing water deliveries to ENP, several minor species in NESRS disappeared (i.e., *Justicia angusta*, *Leersia hexandra*), or their abundance decreased substantially (i.e., *M. capillaris*, *S. lancifolia*, *Dichanthelium* spp.). In contrast, IVs of most NESRS-dominant species increased after six years (i.e., *C. jamaicense*, *E. cellulosa*, *Typha*), with the only exception of *R. tracyi*, whose abundance, after increasing between 2015 and 2018, strongly declined after 2018 (Figure 10).

Changes in species' IVs over time, calculated across each site cluster, allow us to infer whether species moved

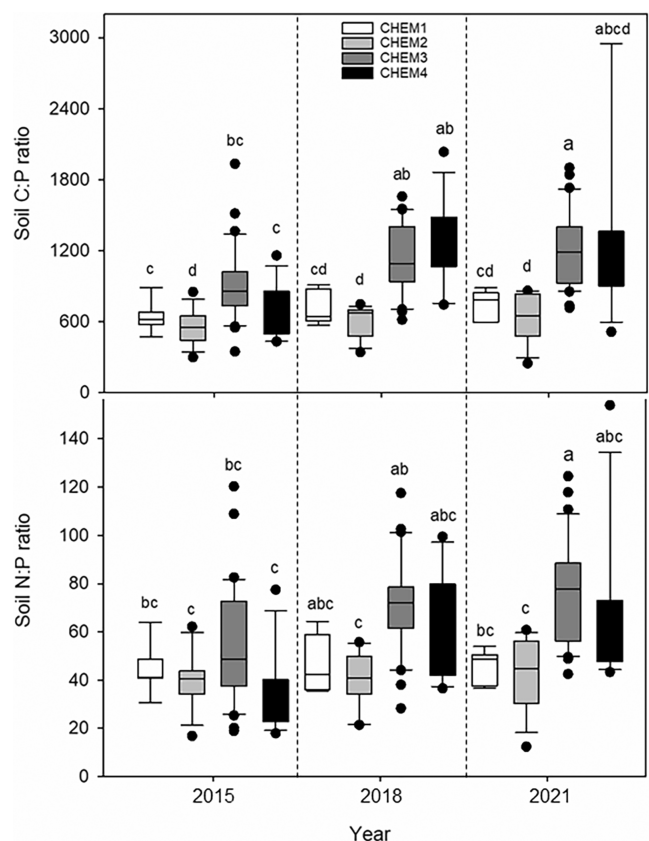


FIGURE 8 Box plot of soil carbon to phosphorus (C:P) and nitrogen to phosphorus (N:P) mass ratios for the three sampling years (2015, 2018, and 2021), summarized by the four site clusters (CHEM1, CHEM2, CHEM3, and CHEM4) identified with the nonmetric multidimensional scaling ordination based on biogeochemical traits of periphyton, floc, and soils. Letters identify significance groupings among site clusters and years at $p \leq 0.05$, based on the results from Welch's one-way ANOVA. See the caption to Figure 7 for an explanation of the features of the box plots.

toward the canal or away from the canal (Figure 10), because we established that CHEM1 and CHEM2 include sites in proximity of the canal, and that CHEM3 and CHEM4 include sites further away from the canal. Shifts in individual species within and among site groups also help demonstrate some of the complexity in landscape-scale response to rehydration. *C. jamaicense* abundance increased in CHEM1, CHEM3, and CHEM4, with the increase mostly occurring after 2018. *E. cellulosa* abundance increased in CHEM1 and CHEM3, and doubled its abundance in CHEM4, both in 2018 and 2021. *R. tracyi* disappeared from CHEM1, CHEM2, and CHEM3, and, after almost doubling its abundance between 2015 and 2018, substantially contracted in CHEM4 in 2021. Similarly to *R. tracyi*, *Panicum hemitomon*, after increasing its abundance threefold between 2015 and 2018, substantially contracted in CHEM4 in 2021. *Typha*

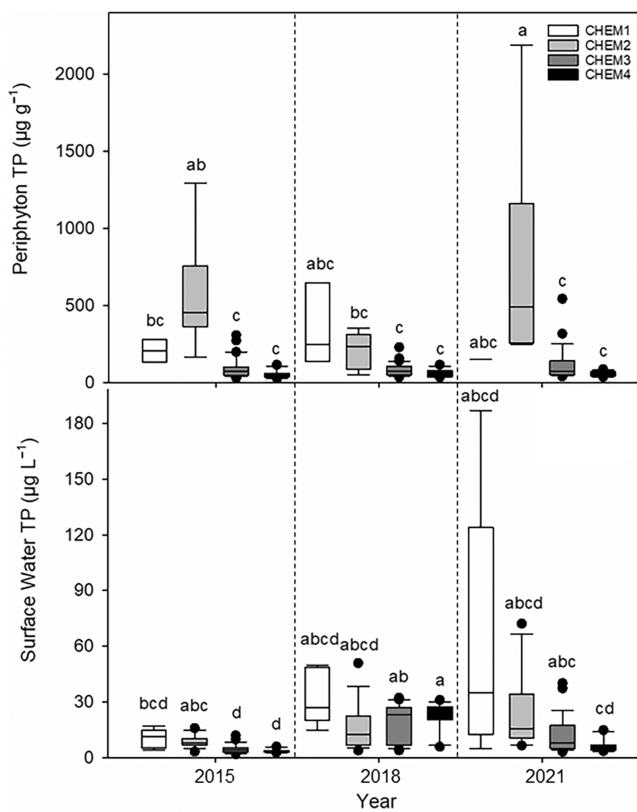


FIGURE 9 Box plot of total phosphorus (TP) concentrations in periphyton and in the surface water for the three sampling years (2015, 2018, and 2021), summarized by the four site clusters (CHEM1, CHEM2, CHEM3, and CHEM4) identified with the nonmetric multidimensional scaling ordination based on biogeochemical traits of periphyton, floc, and soils. Letters identify significance groupings among site clusters and years at $p \leq 0.05$, based on the results from Welch's one-way ANOVA. See the caption to Figure 7 for an explanation of the features of the box plots.

substantially contracted in CHEM1, doubled its abundance in CHEM2, expanded in CHEM3, and did not occur in CHEM4. Hence, in the six years between samplings, we observed *E. cellulosa* steadily expanding to sites further away from the canal, *R. tracyi*, after initially shifting away from the canal, strongly reducing its overall presence in NESRS, and *C. jamaicense* and *Typha* both increasing their abundance, but remaining within the same areas.

From a plant community perspective, we observed that out of four sites characterized by dominant vegetation typical of marl prairies (i.e., *C. jamaicense*, *M. capillaris*, *Rhynchospora microcarpa*, *J. angusta*) in 2015, all belonging to CHEM4, three shifted to vegetation typical of marshes in 2018 (*C. jamaicense*, *R. tracyi*, *P. hemitomon*). After 2018, *C. jamaicense* and *E. cellulosa* succeeded to *R. tracyi* and *P. hemitomon* at these sites. Of the 26, 19, and 15 sites where *C. jamaicense*, *E. cellulosa*,

and *Typha*'s abundance increased between 2015 and 2021, 50%, 37%, and 73%, respectively, burned during the same period. Only 12% of the burned sites did not exhibit any substantial change in vegetation composition, and most of the sites that were affected by fire within the study period burned in 2018, several months before sampling. The burned sites were among those where *E. cellulosa* and *Typha* showed the most significant expansion. Similarly, although *Pontederia cordata*'s IV increased by less than 10% at most of the sites where an increase in its abundance was registered, 80% of these sites burned in 2018.

The NMDS ordination allows us to examine the shifts that occurred in vegetation communities between the three sampling events, and the variability among site clusters (Figure 11). Vegetation composition changed within all site clusters, and CHEM4 sites exhibited the greatest degree of change in both 2018 and 2021. Vegetation in CHEM1 shifted in the direction of decreasing TSLF and increasing hydroperiod. Vegetation in CHEM2 shifted in the direction of decreasing soil N:P ratios. Vegetation in CHEM3 shifted in the direction of increasing hydroperiod. Vegetation in CHEM4 did not shift parallel to any individual environmental variable vector; instead, the changes were driven by a combination of increasing hydroperiod and increasing soil N:P ratios. This interpretation of the NMDS plot is supported by the results of the PERMANOVA analysis, confirming a significant shift in time for wetland vegetation communities, and that hydroperiod and biogeochemistry, and the interaction of these two drivers, explain the variability in NESRS wetland vegetation composition observed during the study period (Table 6).

Species-specific responses to hydrology and chemistry

The indicator species analysis (Table 7) implicates that five species (*R. tracyi*, *M. capillaris*, *Panicum tenerum*, *Dichanthelium* sp., and *R. microcarpa*) are associated with short hydroperiods while two species (*E. cellulosa* and *Typha latifolia*) are associated with longer hydroperiods, that two species (*P. cordata* and *Typha*) are associated with the recent occurrence of fire, and that one species (*R. tracyi*) is associated with extreme oligotrophic conditions (i.e., low soil TN and low soil TP) while one species (*Typha*) is associated with phosphorus enrichment (i.e., low soil N:P ratio and high soil TP). Interestingly, we found the ubiquitous *C. jamaicense* to be associated with medium to high soil TN concentrations, but insensitive to the observed range of soil TP levels.

The indicator species and NMDS analysis reveal the same associations between macrophyte species and abiotic

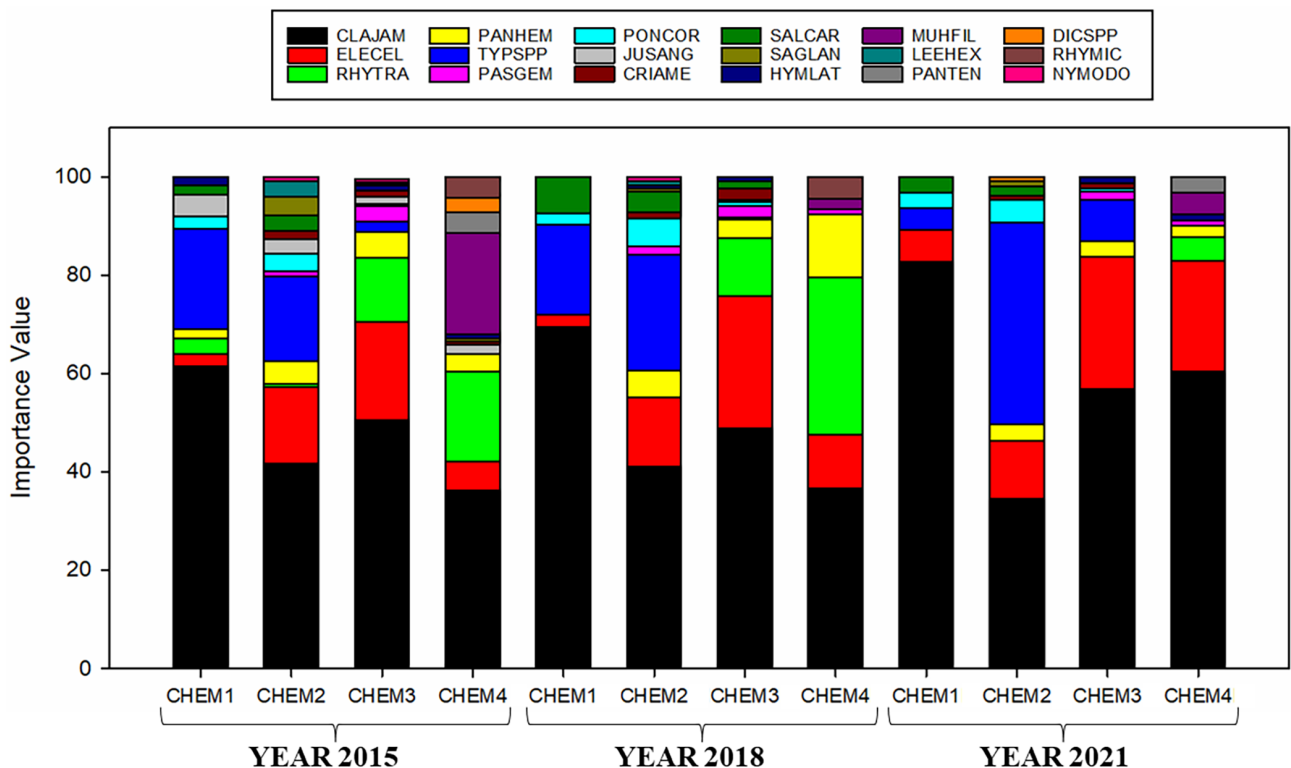


FIGURE 10 Importance values (IVs) calculated for all the species recorded in Northeast Shark River Slough in the sampling years 2015, 2018, and 2021, and included in the analysis, summarized by the four site clusters (CHEM1, CHEM2, CHEM3, and CHEM4) identified with the nonmetric multidimensional scaling ordination based on biogeochemical traits of periphyton, floc, and soils. The IVs were calculated as the sum of the relative frequency (in percentage), relative density (in percentage), and relative biomass (in percentage) of each species within each site cluster divided by 3.

drivers. Both hydroperiod and soil stoichiometry regulate the abundance of the dominant species characterizing the marl prairie or ridge and slough landscapes typical of Everglades wetlands and NESRS (Figures 12 and 13). The abundance of species characterizing marl prairies (*M. capillaris*) decreased along the hydroperiod vector, whereas the abundance of species characterizing sloughs (*E. cellulosa*) increased along the same vector ($p < 0.0001$). Sites characterized by intermediate hydroperiod were coincident with where *R. tracyi* was encountered, while the ubiquitous *C. jamaicense* showed a hump-shaped (unimodal) response along the hydroperiod vector (Figure 12). Conversely, the abundance of *C. jamaicense* increased along the soil N:P ratio vector, whereas the abundance of species typical of moderately oligotrophic environments (*E. cellulosa*) or P-enriched environments (*Typha*) decreased along the same vector (Figure 13).

Figure 14 is a conceptual model that summarizes our results. The model shows ranges in hydroperiod and soil TP concentrations that characterize vegetation communities in NESRS and describes general trends of oligotrophic wetlands in the Everglades. It also includes management recommendations based on findings from key references

(Hagerhey et al., 2008; Lockwood et al., 2003; Newman et al., 2017; Sah et al., 2020). The data used to create the conceptual model are included in Appendix S1: Figure S3.

DISCUSSION

Effects of rehydration and prescribed fire

Our measurements of hydrological, biogeochemical, and vegetation changes during initial stages of Everglades restoration suggest that legacies of prior disturbance are being transformed under the evolving hydrologic conditions. Rehydration has been occurring in response to construction of water structures and changes to operations. Coupled with the application of prescribed fire, rehydration is causing rapid changes in ecosystem components of the affected wetlands that had persistently deviated from the pre-drainage states.

Since 2015, changes in water deliveries to NESRS have expanded the proportion of the landscape experiencing high water depths and long hydroperiods, a trend observed in this study and others (Sarker et al., 2020). We

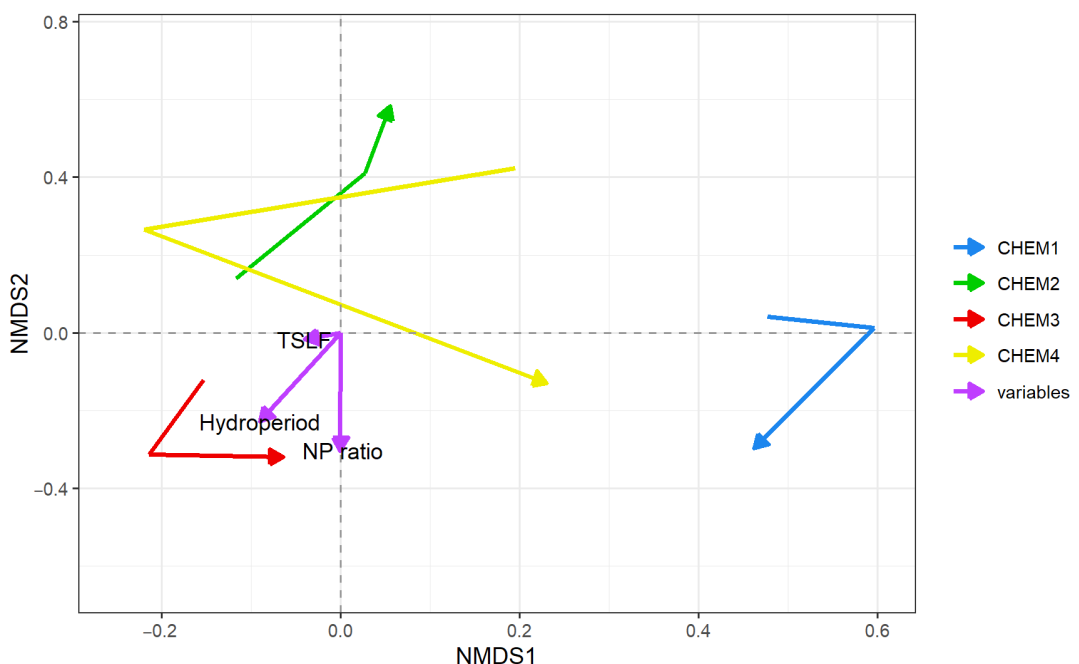


FIGURE 11 Nonmetric multidimensional scaling (NMDS) ordination based on the importance values of plant species observed at the 65 monitoring sites in 2015 (tail of arrows), 2018 (elbow of arrows), and 2021 (tip of arrows). Best solution-stress value corresponded to 0.134. Arrows represent the vegetation shift of each site cluster (CHEM1, CHEM2, CHEM3, and CHEM4), identified with the NMDS ordination based on biogeochemical traits of periphyton, floc, and soils, between the three sampling years. Purple arrows represent the direction and load of environmental variables, which were fitted into the ordination. NP ratio, soil nitrogen:phosphorus mass ratio; TSLF, time since last fire.

TABLE 6 Results from the permutational multivariate analysis of variance, run on the vegetation distance matrix.

Independent variable	SS	R ²	F	p
Year	0.849	0.020	2.347	0.042
Hydroperiod	1.634	0.038	4.522	0.003
Biogeochemistry	5.335	0.124	9.840	0.001
TSLF	0.507	0.012	1.403	0.228
Year × hydroperiod	1.064	0.025	1.961	0.062
Year × biogeochemistry	1.102	0.026	1.016	0.420
Hydroperiod × biogeochemistry	1.441	0.033	1.993	0.029

Note: The analysis was used to test for significant vegetation community shifts in time and to test hydroperiod (i.e., total number of days in a year with soil inundated), biogeochemistry, and time since last fire (TSLF) as ecological drivers (independent variables) of vegetation communities. The effects of some variable interactions were tested as well. The p values reported in boldface denote a statistically significant (<0.05) effect.

also observe a region undergoing distinct biogeochemical shifts associated with both rehydration and fire management. We detected limited signs of P loading in the oligotrophic wetland, and only within subregions (i.e., site clusters) in close proximity to water management infrastructure. Increases in soil stoichiometric ratios (C:P and N:P ratios) were observed that, together with a decrease in soil P concentrations, may indicate re-initiation of peat

accretion in the areas further away from water management infrastructure. These “distant” sites are characterized by shallower soils and lower levels of soil C and nutrients. These are the areas where the magnitude of the hydrologic changes was greatest. We also observed transitions in vegetation communities that seemed to directly result from rehydration and subsequent biogeochemical changes. Plant species requiring drier conditions disappeared or contracted significantly, and were replaced by more hydric species. The expansion of the dominant slough species, *E. cellulosa*, and of *C. jamaicense* into *R. tracyi* marshes and *M. capillaris* prairies following rehydration was facilitated by fire. Similarly, the expansion of *Typha*, which occurred in correspondence with P enrichment, was strongly associated with the occurrence of fire. Increases in soil stoichiometric ratios occurred in parallel to increases in hydroperiod, and their interaction also affected changes in vegetation communities.

Prior to 2015 and NESRS rehydration, soil chemistry and vegetation communities were at a steady state of degraded ridge and slough landscape. This degradation was evidenced by P-enriched soils and widespread presence of short-hydroperiod species in a landscape, which was historically characterized by oligotrophic conditions and long hydroperiods (Appendix S1: Figures S4 and S5). Similarly, data collected between 2006 and 2008 from a

TABLE 7 Results from the multilevel pattern analysis (indicator species analysis).

Species	Group														
	SH	IH	LH	UB	B	RB	LNP	MNP	HNP	LN	MN	HN	LP	MP	HP
CLAJAM	*	*	...	**	**
ELECEL	...	*	*	**	**	...
RHYTRA	***	**	*	***	**	**	...
TYPSPP	...	*	*	...	*	*	***	**	**	***
PASGEM	*	*	...
PONCOR	*	*	*	***
SALCAR	*	*
SAGLAN	**
MUHCAP	***	*	**
LEEHEX	...	*	**
PANTEN	**	*
DICSP	***
RHYMIC	***

Note: Only species that resulted significantly associated with at least one group of sites are included in the table. Sites were grouped separately by duration of hydroperiod, time since last fire, level of soil nitrogen (N):phosphorus (P) ratio, and level of soil total nitrogen and total phosphorus concentrations (SH, short hydroperiod, 0–210 days; IH, intermediate hydroperiod, 211–299 days; LH, long hydroperiod, ≥ 300 days; UB, unburned, TSLF > 5 years; B, burned, TSLF between 2 and 5 years; RB, recently burned, TSLF < 2 years; LNP, low N:P, 0–40; MNP, medium N:P, 40–80; HNP, high N:P, > 80 ; LN, low nitrogen, 0–15 mg g $^{-1}$; MN, medium nitrogen, 15–27 mg g $^{-1}$; HN, high nitrogen, > 27 mg g $^{-1}$; LP, low phosphorus, 0–200 $\mu\text{g g}^{-1}$; MP, medium phosphorus, 200–500 $\mu\text{g g}^{-1}$; HP, high phosphorus, > 500 $\mu\text{g g}^{-1}$). Significant associations: * $p < 0.05$; ** $p < 0.01$; *** $p < 0.001$.

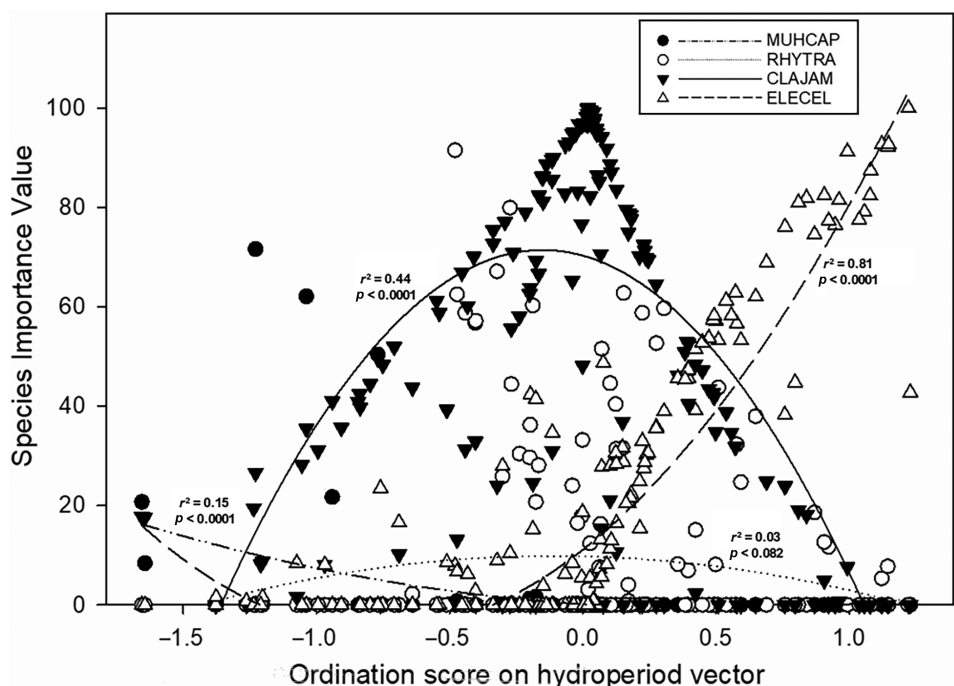


FIGURE 12 Response curve of dominant species modeled on the “hydroperiod” vector in the ordination space. Higher score values correspond to longer hydroperiods. Species were selected because they are representative of Everglades wetland vegetation communities characterized by either short, medium, or long hydroperiods, encountered in the Northeast Shark River Slough region: *Muhlenbergia capillaris* (MUHCAP) prairie, *Rhynchospora tracyi* (RHYTRA) marsh, *Cladium jamaicense* (CLAJAM) marsh, and *Eleocharis cellulosa* (ELECEL) marsh.

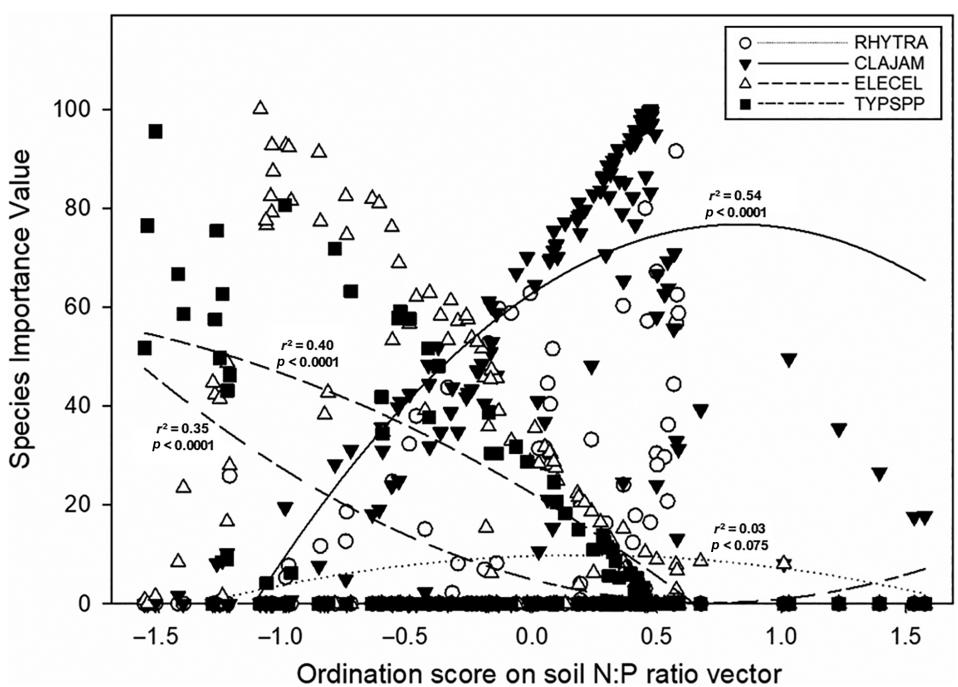


FIGURE 13 Response curve of dominant species modeled on the “soil N:P ratio” vector in the ordination space. Higher score values correspond to higher soil N:P mass ratios. Species were selected because they are representative of Everglades wetland vegetation communities characterized by distinct soil stoichiometric ratios, encountered in the Northeast Shark River Slough region: *Rhynchospora tracyi* (RHYTRA) marsh, *Cladium jamaicense* (CLAJAM) marsh, *Eleocharis cellulosa* (ELECEL) marsh, and *C. jamaicense* and *Typha* (TYPSPP) marsh.

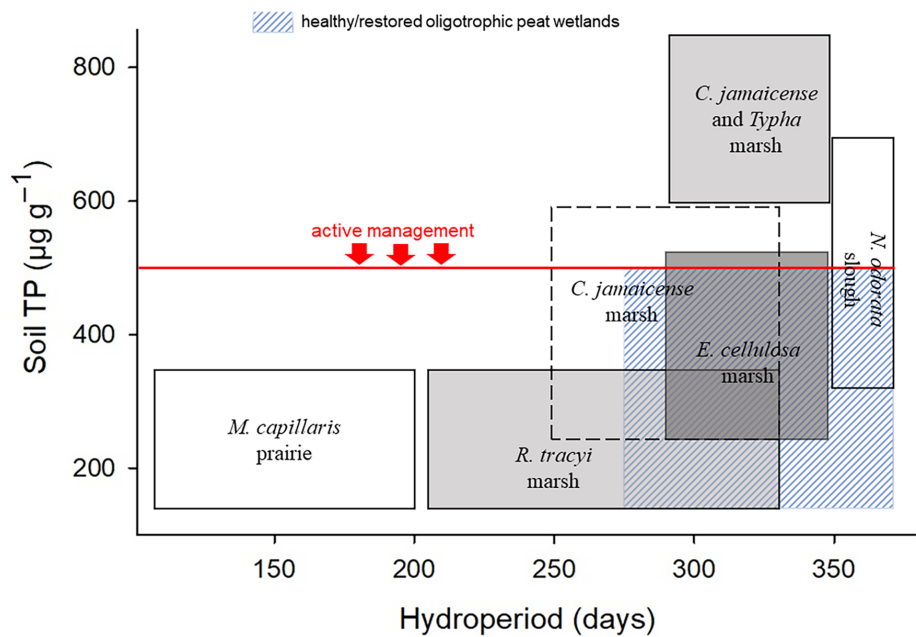


FIGURE 14 Conceptual model showing the control that hydroperiod (i.e., total number of days in a year with soil inundated) and soil total phosphorus (TP) concentration exert in the creation of niches for different Everglades vegetation communities. The hydroperiod and soil TP concentration ranges for each vegetation community class were delineated using the second and third quartiles of the frequency distributions of the two variables in Northeast Shark River Slough. Only hydroperiod and soil TP concentration values corresponding to a significant presence (importance value >5) of the dominant species of each class were included in the estimation of the ranges. Restoration of oligotrophic peat wetlands should aim for hydroperiods longer than 270 days (Lockwood et al., 2003; Sah et al., 2020) and, in degraded landscape patches affected by eutrophication, aim for soil total phosphorus concentrations below $500 \mu\text{g g}^{-1}$ (Hagerthey et al., 2008), by employing the aid of active management strategies such as prescribed fire.

different subset of the monitoring sites situated in NESRS showed steady conditions in terms of eutrophication of soils and macrophyte species composition (Gaiser et al., 2009).

Wetland landscape chemistry variability and trajectories

The ordination technique employed in this study allowed us to identify distinct site clusters in the region characterized by different biogeochemistry, which were also at different distances from the water inflow source. This relationship between wetland biogeochemistry and flow structures highlights how wetland compartmentalization and water management have, over many decades, shaped the ecosystem (McVoy et al., 2011) and modified the baseline conditions at the origin of the distinct biogeochemistry in these subregions.

We observed biogeochemical shifts occurring in the same direction in all subregions, driven by increasing hydroperiods interacting with fire. Although biogeochemistry shifted parallel to increasing hydroperiods in all subregions, we identified some divergent dynamics, due to the distinct baseline conditions and the differences in distance from the water inflow source. While at some sites in proximity of the canal we observed P enrichment, which was mostly expressed in the periphyton matrix, at sites further away from the canal we observed decreases in soil and floc P concentrations and increases in soil C:P and N:P ratios. Considering that these latter sites are characterized by shallow soils with low soil C concentrations, we hypothesize that they might have started accreting peat because of the recent extension of hydroperiods, which exert the strongest control over peat accretion (Craft & Richardson, 1993). Peat accretion might be in fact causing incremental annual accumulation of soil C and N stocks, while diluting soil P concentrations.

Although marsh surface water TP concentrations increased in 2018 and 2021 compared with 2015, surface water TP concentrations in the canal did not change throughout the study period, and, at many sites, were below the protective inflow long-term target of $8 \mu\text{g L}^{-1}$. Sarker et al. (2020) suggested these increases in marsh surface water TP concentration after rehydration were related to internal legacy P loading. Provided that the water delivered to NESRS stays at present levels, the continuation of restorative water flows into NESRS may slowly relieve, over the long term, the wetland landscape of legacy P, as it dissolves from enriched patches into the surface water and is widely absorbed in the landscape. Davis et al. (2018) provided one example of how nutrients

dissolved in the surface water can move across the long-hydroperiod wetland landscape through lateral flow.

Vegetation community transitions and potential trajectories

After six years of hydrologic restoration, vegetation communities have become more similar between site clusters, as hydrologic conditions have become more homogeneous. Only vegetation in one site cluster that is in close proximity to the water inflow source (CHEM2) became more dissimilar, despite hydrology shifting in parallel to the other three subregions. The increase in dissimilarity in this particular subregion was driven by P enrichment and fire occurrence interacting with a degraded state characterized by a significant presence of invasive macrophyte species. Hence, while hydrology was the dominant driver of vegetation communities shifts at the landscape scale, biogeochemistry and fire occurrence were critical drivers of vegetation communities at the scale of individual landscape patches (Foti et al., 2012).

It is important to note that the direction and rate of vegetation change depend on the magnitude of the hydrologic alteration (Armentano et al., 2006; Sah et al., 2014; Zweig & Kitchens, 2008). Although rehydration started in 2015, new bridges were completed in 2018 and the strategy for water deliveries to NESRS has evolved since the beginning of rehydration, increasing the magnitude of the hydrologic alteration. Previous studies in nearby wetlands found that changes between vegetation types happened within four years when the hydrological transition is from drier to wetter conditions (Armentano et al., 2006; Zweig & Kitchens, 2008). Nonetheless, the increasing magnitude of the hydrologic alteration has promoted a continuous evolution of vegetation communities in this region, beyond the first four years of rehydration.

The most evident vegetation change we observed in the first three years of wetland restoration was the disappearance or contraction of several minor short-hydroperiod species typical of the prairie vegetation community type. In floodplain wetlands of southern Australia that were also rehydrated after degradation due to decades of anthropogenic drying, aquatic plant coverage increased to the detriment of terrestrial plants (Alexander et al., 2008). In addition, dominant species typical of marsh and slough communities expanded throughout the NESRS wetland landscape. At sites further away from the water inflow, where prairie habitats had evolved due to anthropogenic drying of the historic ridge and slough marshes, we observed two phases of succession in vegetation communities. After three years

of rehydration, macrophyte species that prefer intermediate hydroperiod conditions (i.e., *R. tracyi* and *P. hemitomon*) succeeded short-hydroperiod prairie species, while, after six years and following additional changes in operations that increased the magnitude of water deliveries, these species were replaced by long-hydroperiod species (i.e., *C. jamaicense* and *E. cellulosa*). In one of the site clusters (CHEM2), *Typha*'s abundance increased substantially, while the abundance of other dominant long-hydroperiod species decreased. This was the sub-region with the highest occurrence of fire, and it is where signs of P enrichment were detected. Regardless, *C. jamaicense* and *E. cellulosa* expanded throughout the rest of the landscape. The observed shifts are clearly a result of the hydrologic changes that occurred following rehydration. For example, *R. tracyi* flats and extensive *P. hemitomon* flats disappeared from Everglades southern WCA 3A due to extended inundation following impoundment (Zweig & Kitchens, 2008), whereas increases in *E. cellulosa* appear to be a result of extended hydroperiods and increased water depths (Appendix S1: Table S3; Childers et al., 2006). A shift in vegetation communities along the hydroperiod vector has also been observed in Everglades Taylor Slough following increased water deliveries (Sah et al., 2014). We hypothesize that in the future, because of the complete disappearance of minor prairie species, and a further expansion of species adapted to extended hydroperiods, wetland rehydration will translate in vegetation communities continuing to shift toward higher similarity in this region.

Differences in ecology and morphological traits make some species better indicators of transitions between vegetation communities occurring in the short or long term in response to rehydration. For example, *C. jamaicense* is a rhizomatous plant that can survive extended droughts but exhibit unique responses under different drought durations. In contrast, *E. cellulosa* is characterized by an herbaceous growth structure and can exhibit rapid responses to hydrologic alterations and was therefore identified as a short-term sentinel species of wetland community change (Zweig & Kitchens, 2008). In our study, *C. jamaicense* expanded only in the second half of the study period, while *E. cellulosa* and *R. tracyi* quickly changed relative abundance and were therefore short-term sentinels of vegetation transitions resulting from rehydration.

While fire seems to have supported the initial establishment of slough communities in the areas further away from water inflow by leaving open water available for *E. cellulosa* colonization (Armentano et al., 2006), it seems to have also supported the expansion of *Typha* at several sites near the canal, and of other high

P-demanding species (i.e., *P. cordata*). This suggests that the large prescribed fire carried out during the 2018 dry season was not effective in the short term at reducing the abundance of *Typha*. Fire disturbances, by leaving open spaces, can provide a competitive advantage to plants with rapid vegetative growth and aerial seed dispersal, such as *Typha* (Newman et al., 1998). Possibly, the intensity of the fire was not high enough to induce mortality of the invasive species (Trouvé et al., 2021). However, prescribed burns need to occur when surface water is present in order to protect peat soils. By implementing this strategy, rhizomes of *Typha* are protected as well, insuring its survival (Apfelbaum, 1985). Prescribed fires applied when surface water depths are still relatively low but high enough to support flow might be more effective in dispersing the P-rich ashes from the burned invasive macrophytes through lateral flow of surface water (Davis et al., 2018; Nocentini, Kominoski, & Sah, 2021). For example, part of the P released by the Everglades Mustang Corner fire in summer 2008 was reported to have traveled about 24 km southward when water depths were between 20 and 30 cm (Davis et al., 2018). This approach, consistently and repeatedly implemented for a long period of time, could possibly reduce eutrophication of the areas characterized by thick vegetation plumes.

Overall, invasive species are very persistent regardless of burn treatments and can take advantage of a variety of ecological conditions (Newman et al., 1996), which can result from site-specific history (Newman et al., 1998). In addition, for the specific case of degraded Everglades vegetation communities with a substantial presence of invasive *Typha*, a C cycling feedback loop has been described. This loop is reinforced by extensive eutrophication, where increased vegetation nutrient content translates to increased decomposition rates in the soil, lower peat accretion rates, and increased relative content of mineralized nutrients in the soil (Newman et al., 2017).

Species response to ecological drivers

The association of both dominant and minor macrophyte species within specific ranges of hydroperiod, soil nutrient concentrations, and soil stoichiometric ratios corroborated the significance of these environmental variables in driving wetland vegetation community dynamics (Sah et al., 2014).

The relative abundance of dominant plant species either increased, decreased, or showed unimodal responses to variations in hydroperiod and soil N:P ratios. Increases in hydroperiod are causing shifts in species composition, as many wetland species (e.g., *C. jamaicense*) need a certain number of days with no standing water for successful

seedling recruitment (Keddy & Ellis, 1985), while other species, such as *E. cellulosa*, thrive with continuous inundation (Childers et al., 2006). Prairie species such as *M. capillaris* need short hydroperiods and were replaced by more hydric species. Resource availability, which, in many cases, is effectively represented by C:N:P stoichiometry, has been established as a fundamental driver of wetland community types, including their composition and structure (Bedford et al., 1999; Vermeer & Berendse, 1983). In NESRS, the dominant macrophyte species appear to have distinct niches related to N:P stoichiometry, oscillating between species that prefer higher proportion of soil N (e.g., *C. jamaicense*) and those that prefer a higher proportion of soil P (e.g., *R. tracyi*, *M. capillaris*, *Typha*). However, native species associated with low soil N:P ratios were also associated with low soil N concentrations (e.g., *M. capillaris*), while invasive species associated with low soil N:P ratios were also associated with high soil P concentrations (e.g., *Typha* and *S. caroliniana*). This is in line with most Everglades native species historically inhabiting an oligotrophic ecosystem characterized by low P levels (Davis & Ogden, 1994).

Potential trajectories of wetland restoration

Understanding the capacity of degraded ecosystems undergoing restoration to recover is necessary to determine ecological benchmarks for restoration (Gunderson, 2001; Newman et al., 2017; Sklar et al., 2005). Monitoring changes in water, periphyton and soil chemistry, and plant communities' composition and structure during the initial phases of Everglades wetland restoration allowed us to analyze a system clearly in a transitional state, but from which we could identify some clear trajectories.

Shifts in biogeochemistry and vegetation were more significant at wetlands further away from water inflow. These southern wetlands had been more hydrologically compromised, showing relatively dry conditions in comparison with the historical wetter habitats. So, the effects of rehydration have manifested in these wetlands as re-initiation of peat accretion, and as disappearance or contraction of less flood-tolerant species. Wetlands in proximity of the water inflow source did not change as much, as hydrologic changes in these wetlands were less dramatic, and these sites were already characterized by deep peat soils and high nutrient concentrations. Even though wetlands in proximity of the water inflow source are hydrologically closer to restored conditions, the biological progression toward a restored state seems to be prevented by the feedbacks established between P-enriched soils and the invasive macrophyte *Typha*.

Hence, if for the wetlands further away from the water inflow structures one of the goals of restoration is to pass a peat accumulation threshold, which is achieved by increasing the length of inundation, wetlands in proximity of the water inflow source will need consistent management intervention to reverse the degraded conditions caused by a history of eutrophication. We hypothesize that fire is one important management tool to help reduce the presence of thick vegetation plumes, but only if applied with ambient conditions that enable the expression of fire intensity regimes capable of reducing eutrophication. Reducing eutrophication and the related vegetation plumes would help reestablishing marsh connectivity, water flow velocities, and, subsequently, microtopography (Harvey et al., 2017; Larsen et al., 2011).

The overall loss of plant richness observed, which mostly occurred in the wetlands further away from the water inflow, should not be interpreted as a negative impact of restoration. Instead, diversity objectives should rather focus on restoring the slough, ridge, and tree island habitat diversity (Armentano et al., 2006), which we believe will confer high rates of plant species diversity within daily movement ranges of most mobile organisms. We observed a transition from *M. capillaris* prairie communities to marsh communities characterized, initially, by *C. jamaicense*, *R. tracyi*, and *P. hemitomon*, and, after, by *C. jamaicense* and *E. cellulosa*. We also observed the beginning of a transition from marsh to slough communities, characterized by the expansion of *E. cellulosa* throughout the wetland landscape, driven by rehydration, and facilitated by fire. Similar dynamics have been reported in the past after changes to hydrologic operations in Everglades Taylor Slough (Armentano et al., 2006; Sah et al., 2014). In contrast, while regime shifts from oligotrophic *C. jamaicense* marsh or *N. odorata* slough to *Typha* marsh, driven by eutrophication, have been previously described (Gunderson, 2001; Hagerthey et al., 2008), we did not observe any sign of a transition from *C. jamaicense*-*Typha* marsh, formed because of past eutrophication, back to a native ridge or slough community. Nonetheless, we recognize that the *C. jamaicense*-*Typha* marsh represents an intermediate step between a *C. jamaicense* ridge regime and a *Typha* regime, the latter of which is an expression of maximum eutrophication. The *C. jamaicense*-*Typha* marsh in NESRS was characterized by soil TP concentrations between 600 and 900 $\mu\text{g g}^{-1}$. Supporting our observations, in Everglades WCA2, the *Typha* regime was reached at soil TP concentrations above 1000 $\mu\text{g g}^{-1}$, while the *C. jamaicense* ridge regime was occurring with soil TP concentrations below 500 $\mu\text{g g}^{-1}$ (Hagerthey et al., 2008). Implementation of water quality improvement features associated with the federal consent decree

in the 1990s has probably prevented further eutrophication of NESRS and a dreaded shift to a *Typha* regime.

Wetland ecosystem dynamics between degraded and restored conditions along the ecological trajectory can be difficult to predict as they are often characterized by nonlinear responses (Hagerhey et al., 2008; Zweig & Kitchens, 2009). From our analysis, it appears clear that the NESRS wetlands are presently in a transient state, as the vegetation shifts caused by the evolving hydrologic alterations are still occurring. On the other hand, the *C. jamaicense*–*Typha* marsh, indicative of degraded conditions, has not been perturbed yet by rehydration and the use of prescribed fire. Our results suggest that it could possibly be reversed either (1) by relieving legacy P in the long term (hypothetically, decades), with the increasing magnitude of the hydrologic alteration, and provided that unenriched water is delivered to the region, or, (2) more realistically and in a relatively shorter time, by coupling the hydrologic alteration with distinct active management practices that will specifically target the removal of excessive soil nutrients, the removal of invasive vegetation, and the recreation of the original microtopography. Finally, the time needed to trigger detectable reversal and the necessary set of restoration actions to be employed will vary depending on the targeted landscape patch: the more extensive the P enrichment and the larger the degraded patch, the stronger the feedback loops and the resistance to restoration (Newman et al., 2017; Suding et al., 2004).

To advance critically needed restoration of wetlands and freshwater ecosystems, future research should: (1) analyze the vegetation community dynamics over longer time periods of restored hydrology to better understand how the rate and pace of vegetation trajectories are influenced by incremental restoration actions; (2) measure peat soil accretion rates and the related changes in soil elemental stoichiometry following rehydration of degraded wetlands; (3) explore how fire seasonality and fire intensity thresholds can be effectively used to reduce eutrophication, and support a transition from plumes of thick vegetation, inhabited by invasive species, to ridge and slough communities, facilitating the reestablishment of the original wetland topographic mosaic.

ACKNOWLEDGMENTS

This research was supported by multiple cooperative and task agreements between Florida International University and Everglades National Park (CA H5297-05-0099, P11A50510, P14AC01639, P16AC00032, and P16AC01704). This material was developed in collaboration with the Florida Coastal Everglades Long-Term Ecological Research program under National Science Foundation Grant No. DEB-9910514 (for work from 2000 to 2006), Grant No. DBI-0620409 (for work from 2007 to 2012), Grant No.

DEB-1237517 (for work from Dec. 2012 to 2018). We thank Franco Tobias, Rafael Travieso, Michael Kline, Michelle Robinson, Diana Johnson, Sanku Dattamudi, Saoli Chandra, Mary Zeller, Sean Charles, Shishir Sarker, Andy Bramburger, Jay Munyon, and Kenneth Anderson for field and laboratory assistance. This is contribution 1677 from the Institute of Environment at Florida International University.

CONFLICT OF INTEREST STATEMENT

The authors declare no conflicts of interest.

DATA AVAILABILITY STATEMENT

Data (Hoffman, Rizzie, Nocentini, Sarker, et al., 2021; Hoffman, Rizzie, Nocentini, Tobias, et al., 2021) are available from the Environmental Data Initiative Data Portal: <https://doi.org/10.6073/pasta/8af4f2a4e37b209934c12f11a1d5866b> and <https://doi.org/10.6073/pasta/73e4219fef685927c24140250deb6f1b>.

ORCID

Andrea Nocentini  <https://orcid.org/0000-0001-7848-1025>

Jed Redwine  <https://orcid.org/0000-0001-8952-2136>

Evelyn Gaiser  <https://orcid.org/0000-0003-2065-4821>

Troy Hill  <https://orcid.org/0000-0003-2980-4099>

Sophia Hoffman  <https://orcid.org/0000-0003-1197-8648>

John S. Kominoski  <https://orcid.org/0000-0002-0978-3326>

Jay Sah  <https://orcid.org/0000-0003-3891-6041>

REFERENCES

Alexander, P., D. L. Nielsen, and D. Nias. 2008. "Response of Wetland Plant Communities to Inundation within Floodplain Landscapes." *Ecological Management & Restoration* 9: 187–195.

Apfelbaum, S. I. 1985. "Cattail (*Typha* spp.) Management." *Natural Areas Journal* 5: 9–17.

Armentano, T. V., J. P. Sah, M. S. Ross, D. T. Jones, H. C. Cooley, and C. S. Smith. 2006. "Rapid Responses of Vegetation to Hydrological Changes in Taylor Slough, Everglades National Park, Florida, USA." *Hydrobiologia* 569: 293–309.

Bedford, B. L., M. R. Walbridge, and A. Aldous. 1999. "Patterns in Nutrient Availability and Plant Diversity of Temperate North American Wetlands." *Ecology* 80: 2151–69.

Bricker, S. B., B. Longstaff, W. Dennison, A. Jones, K. Boicourt, C. Wicks, and J. Woerner. 2008. "Effects of Nutrient Enrichment in the Nation's Estuaries: A Decade of Change." *Harmful Algae* 8: 21–32.

Chiang, C., C. B. Craft, D. W. Rogers, and C. J. Richardson. 2000. "Effects of 4 Years of Nitrogen and Phosphorus Additions on Everglades Plant Communities." *Aquatic Botany* 68: 61–78.

Childers, D. L., D. Iwaniec, D. Rondeau, G. Rubio, E. Verdon, and C. J. Madden. 2006. "Responses of Sawgrass and Spikerush to Variation in Hydrologic Drivers and Salinity in Southern Everglades Marshes." *Hydrobiologia* 569: 273–292.

Clarke, K. R. 1993. "Non-Parametric Multivariate Analyses of Changes in Community Structure." *Australian Journal of Ecology* 18: 117–143.

Cole, C. A., R. P. Brooks, and D. H. Wardrop. 1997. "Wetland Hydrology as a Function of Hydrogeomorphic (HGM) Subclass." *Wetlands* 17: 456–467.

Craft, C. B., and C. J. Richardson. 1993. "Peat Accretion and N, P, and Organic C Accumulation in Nutrient-Enriched and Unenriched Everglades Peatlands." *Ecological Applications* 3: 446–458.

Craft, C. B., J. Vymazal, and C. J. Richardson. 1995. "Response of Everglades Plant Communities to Nitrogen and Phosphorus Additions." *Wetlands* 15: 258–271.

Davis, S., and J. C. Ogden. 1994. *Everglades: The Ecosystem and Its Restoration*. Delray Beach, FL: St. Lucie Press.

Davis, S. E., R. Boucek, E. Castañeda-Moya, S. Dessu, E. Gaiser, J. Kominoski, J. P. Sah, D. Surratt, and T. Troxler. 2018. "Episodic Disturbances Drive Nutrient Dynamics along Freshwater-to-Estuary Gradients in a Subtropical Wetland." *Ecosphere* 9: e02296.

De Cáceres, M., F. Jansen, and M. M. De Cáceres. 2016. "Package 'Indicspecies' (Version 1.7.6)." <http://cran.r-project.org/web/packages/indicspecies/indicspecies.pdf>.

Foti, R., M. del Jesus, A. Rinaldo, and I. Rodriguez-Iturbe. 2012. "Hydroperiod Regime Controls the Organization of Plant Species in Wetlands." *Proceedings of the National Academy of Sciences of the United States of America* 109: 19596–600.

Gaiser, E. E., P. V. McCormick, S. E. Hagerth, and A. D. Gottlieb. 2011. "Landscape Patterns of Periphyton in the Florida Everglades." *Critical Reviews in Environmental Science and Technology* 41: 92–120.

Gaiser, E. E., L. Scinto, J. Trexler, D. Johnson, and F. Tobias. 2009. "Developing Ecosystem Response Indicators to Hydrologic and Nutrient Modifications in Northeast Shark River Slough, Everglades National Park." Final Report to Everglades National Park, May 30, 2009, Homestead, USA.

Gaiser, E. E., J. C. Trexler, J. H. Richards, D. L. Childers, D. Lee, A. L. Edwards, L. J. Scinto, K. Jayachandran, G. B. Noe, and R. D. Jones. 2005. "Cascading Effects of Low-Level Phosphorus Enrichment in the Florida Everglades." *Journal of Environmental Quality* 34: 717–723.

Gunderson, L. H. 1994. "Vegetation of the Everglades: Determinants of Community Composition." In *Everglades: The Ecosystem and Its Restoration*, edited by S. Davis and J. C. Ogden, 323–340. Delray Beach, FL: St. Lucie Press.

Gunderson, L. H. 2001. "Managing Surprising Ecosystems in Southern Florida." *Ecological Economics* 37: 371–78.

Hagerth, S. E., S. Newman, K. Rutcher, E. P. Smith, and J. Godin. 2008. "Multiple Regime Shifts in a Subtropical Peatland: Community-Specific Thresholds to Eutrophication." *Ecological Monographs* 78: 547–565.

Harvey, J. W., P. R. Wetzel, T. E. Lodge, V. C. Engel, and M. S. Ross. 2017. "Role of a Naturally Varying Flow Regime in Everglades Restoration." *Restoration Ecology* 25: S27–S38.

Hobbs, R. J., S. Arico, J. Aronson, J. S. Baron, P. Bridgewater, V. A. Cramer, P. R. Epstein, et al. 2006. "Novel Ecosystems: Theoretical and Management Aspects of the New Ecological World Order." *Global Ecology and Biogeography* 15: 1–7.

Hoffman, S., C. B. Rizzie, A. Nocentini, S. Sarker, J. S. Kominoski, E. Gaiser, and L. Scinto. 2021. "Biogeochemical Data Collected from Northeast Shark River Slough, Everglades National Park, Florida, Ongoing since 2006 ver 6." Environmental Data Initiative. <https://doi.org/10.6073/pasta/8af4f2a4e37b209934c12f11a1d5866b>.

Hoffman, S., C. B. Rizzie, A. Nocentini, F. Tobias, J. S. Kominoski, and E. Gaiser. 2021. "Vegetation Data Collected from Northeast Shark River Slough, Everglades National Park, Florida, from September 2006 to Present ver 6." Environmental Data Initiative. <https://doi.org/10.6073/pasta/73e4219fef685927c24140250deb6f1b>.

Hu, T., J. Liu, G. Zheng, D. Zhang, and K. Huang. 2020. "Evaluation of Historical and Future Wetland Degradation Using Remote Sensing Imagery and Land Use Modeling." *Land Degradation & Development* 31: 65–80.

Hurteau, M. D., and M. L. Brooks. 2011. "Short- and Long-Term Effects of Fire on Carbon in US Dry Temperate Forest Systems." *BioScience* 61: 139–146.

Keddy, P. A., and T. H. Ellis. 1985. "Seedling Recruitment of 11 Wetland Species along a Water Level Gradient: Shared or Distinct Responses?" *Canadian Journal of Botany* 63: 1876–79.

Kominoski, J. S., M. Fernandez, P. Breault, V. Slater, and B. B. Rothermel. 2022. "Fire Severity and Post-Fire Hydrology Drive Nutrient Cycling and Plant Community Recovery in Intermittent Wetlands." *Ecosystems* 25: 265–278.

Larsen, L. G., N. Aumen, C. Bernhardt, V. Engel, T. Givnish, S. Hagerth, J. Harvey, et al. 2011. "Recent and Historic Drivers of Landscape Change in the Everglades Ridge, Slough, and Tree Islands Mosaic." *Critical Reviews in Environmental Science and Technology* 41: 344–381.

Larsen, L. G., J. W. Harvey, and J. P. Crimaldi. 2009. "Morphologic and Transport Properties of Natural Organic Floc." *Water Resources Research* 45: W01410.

Li, X., R. Bellerby, C. Craft, and S. E. Widney. 2018. "Coastal Wetland Loss, Consequences, and Challenges for Restoration." *Anthropocene Coasts* 1: 1–15.

Light, S. S., and J. W. Dineen. 1994. "Water Control in the Everglades: A Historical Perspective." In *Everglades: The Ecosystem and Its Restoration*, edited by S. Davis and J. C. Ogden, 47–84. Delray Beach, FL: St. Lucie Press.

Lockwood, J. L., M. S. Ross, and J. P. Sah. 2003. "Smoke on the Water: The Interplay of Fire and Water Flow on Everglades Restoration." *Frontiers in Ecology and the Environment* 1: 462–68.

LoSchiavo, A. J., R. G. Best, R. E. Burns, S. Gray, M. C. Harwell, E. Hines, A. R. McLean, T. St. Clair, S. Traxler, and J. W. Vearil. 2013. "Lessons Learned from the Adaptive Management in Comprehensive Everglades Restoration." *Ecology and Society* 18: 70.

McVoy, C., W. Park Said, J. Obeysekera, J. VanArman, and T. Dreschel. 2011. *Landscapes and Hydrology of the Pre-Drainage Everglades*. Gainesville, FL: University Press of Florida.

Meng, B., J. Liu, K. Bao, and B. Sun. 2020. "Methodologies and Management Framework for Restoration of Wetland Hydrologic Connectivity: A Synthesis." *Integrated Environmental Assessment and Management* 16(438): 451.

National Research Council. 2018. *Progress towards Restoring the Everglades: The Seventh Biennial Review*. Washington DC: National Academies Press.

Newman, S., J. B. Grace, and J. W. Koebel. 1996. "Effects of Nutrients and Hydroperiod on *Typha*, *Cladium*, and *Eleocharis*: Implications for Everglades Restoration." *Ecological Applications* 6: 774–783.

Newman, S., T. Z. Osborne, S. E. Hagerthey, C. Saunders, K. Rutchez, T. Schall, and K. R. Reddy. 2017. "Drivers of Landscape Evolution: Multiple Regimes and Their Influence on Carbon Sequestration in a Sub-Tropical Peatland." *Ecological Monographs* 87: 578–599.

Newman, S., J. Schuette, J. B. Grace, K. Rutchez, T. Fontaine, K. R. Reddy, and M. Pietrucha. 1998. "Factors Influencing Cattail Abundance in the Northern Everglades." *Aquatic Botany* 60: 265–280.

Nocentini, A., J. S. Kominoski, J. J. O'Brien, and J. Redwine. 2022. "Fire Intensity and Ecosystem Oligotrophic Status Drive Relative Phosphorus Release and Retention in Freshwater Marshes." *Ecosphere* 13: e4263.

Nocentini, A., J. S. Kominoski, and J. P. Sah. 2021. "Interactive Effects of Hydrology and Fire Drive Differential Biogeochemical Legacies in Subtropical Wetlands." *Ecosphere* 12: e03408.

Nocentini, A., J. S. Kominoski, J. P. Sah, J. Redwine, M. Gue, I. Wilson-Navarro, and A. Gil. 2021. "Prescribed Fires inside Everglades National Park (Florida, United States)." *Bulletin of the Ecological Society of America* 102: e01872.

Noe, G. B., and D. L. Childers. 2007. "Phosphorus Budgets in Everglades Wetland Ecosystems: The Effects of Hydrology and Nutrient Enrichment." *Wetlands Ecology and Management* 15: 189–205.

Ojima, D. S., D. S. Schimel, W. J. Parton, and C. E. Owensby. 1994. "Long- and Short-Term Effects of Fire on Nitrogen Cycling in Tallgrass Prairie." *Biogeochemistry* 24: 67–84.

Osborne, T. Z., G. L. Bruland, S. Newman, K. R. Reddy, and S. Grunwald. 2011. "Spatial Distributions and Eco-Partitioning of Soil Biogeochemical Properties in the Everglades National Park." *Environmental Monitoring and Assessment* 183: 395–408.

Osborne, T. Z., L. N. Kobziar, and P. W. Inglett. 2013. "Fire and Water: New Perspectives on Fire's Role in Shaping Wetland Ecosystems." *Fire Ecology* 9: 1–5.

R Core Team. 2022. *R: A Language and Environment for Statistical Computing*. Vienna: R Foundation for Statistical Computing. <http://www.R-project.org/>.

Richards, J. H., and C. T. Ivey. 2004. "Morphological Plasticity of *Sagittaria lancifolia* in Response to Phosphorus." *Aquatic Botany* 80: 53–67.

Ruiz, P. L., J. P. Sah, M. S. Ross, and A. A. Spitzig. 2013. "Tree Island Response to Fire and Flooding in the Short-Hydroperiod Marl Prairie Grasslands of the Florida Everglades, USA." *Fire Ecology* 9: 38–54.

Sah, J. P., M. S. Ross, C. Pulido, S. Stoffella, and R. Vidales. 2020. "Landscape Pattern-Marl Prairie/Slough Gradient; Patterns and Trends in Shark Slough Marshes and Associated Marl Prairies." Year 5 Report, submitted to U.S. Army Engineer Research and Development Center (U.S. Army – ERDC), Jacksonville, USA.

Sah, J. P., M. S. Ross, P. L. Ruiz, J. R. Snyder, D. Rodriguez, and W. T. Hilton. 2011. "Cape Sable Seaside Sparrow Habitat Monitoring and Assessment." Final Report 2010, Submitted to U.S. Army Engineer Research and Development Center (U.S. Army – ERDC), Jacksonville, USA.

Sah, J. P., M. S. Ross, S. Sah, P. Minchin, and J. Sadle. 2014. "Trajectories of Vegetation Responses to Water Management in Taylor Slough, Everglades National Park, Florida." *Wetlands* 34: S65–S79.

Sah, J. P., M. S. Ross, J. R. Snyder, S. Stoffella, A. Jirout, R. Vidales, and J. Blanco. 2016. "Re-Sampling of Vegetation Survey Sites within Cape Sable Seaside Sparrow Habitat." Task Agreement # P15AC01254. Cooperative Agreement # H5000-10-0104. Submitted to South Florida Natural Resources Center, Everglades and Dry Tortugas National Parks, Homestead, USA.

Sarker, S. K., J. S. Kominoski, E. E. Gaiser, L. J. Scinto, and D. T. Rudnick. 2020. "Quantifying Effects of Increased Hydroperiod on Wetland Nutrient Concentrations during Early Phases of Freshwater Restoration of the Florida Everglades." *Restoration Ecology* 28: 1561–73.

Scheffer, M., and S. R. Carpenter. 2003. "Catastrophic Regime Shifts in Ecosystems: Linking Theory to Observation." *Trends in Ecology & Evolution* 18: 648–656.

Seastedt, T. R., R. J. Hobbs, and K. N. Suding. 2008. "Management of Novel Ecosystems: Are Novel Approaches Required?" *Frontiers in Ecology and the Environment* 6: 547–553.

Sklar, F. H., M. J. Chimney, S. Newman, P. McCormick, D. Gawlik, L. Miao, C. McVoy, et al. 2005. "The Ecological-Societal Underpinnings of Everglades Restoration." *Frontiers in Ecology and the Environment* 3: 161–69.

Sklar, F. H., E. Cline, M. Cook, T. Dreschel, C. Coronado, and D. E. Gawlik. 2008. *South Florida Environmental Report. Chapter 6: Ecology of the Everglades Protection Area*. West Palm Beach, FL: South Florida Water Management District.

Slocum, M. G., W. J. Platt, B. Beckage, B. Panko, and J. B. Lushine. 2007. "Decoupling Natural and Anthropogenic Fire Regimes: A Case Study in Everglades National Park, Florida." *Natural Areas Journal* 27(1): 41–55.

Smith, T. J., III, A. M. Foster, and J. W. Jones. 2015. *Fire History of Everglades National Park and Big Cypress National Preserve, Southern Florida*. Open File Report 2015-1034. Reston, VA: U.S. Department of the Interior, U.S. Geological Survey.

Solórzano, L., and J. H. Sharp. 1980. "Determination of Total Dissolved P and Particulate P in Natural Waters." *Limnology and Oceanography* 25: 754–58.

Suding, K. N., K. L. Gross, and G. R. Houseman. 2004. "Alternative States and Positive Feedbacks in Restoration Ecology." *Trends in Ecology & Evolution* 19: 46–53.

Surratt, D., D. Shinde, and N. Aumen. 2012. "Recent Cattail Expansion and Possible Relationships to Water Management: Changes in Upper Taylor Slough (Everglades National Park, Florida, USA)." *Environmental Management* 49: 720–733.

Trouvé, R., L. Osborne, and P. J. Baker. 2021. "The Effect of Species, Size, and Fire Intensity on Tree Mortality within a Catastrophic Bushfire Complex." *Ecological Applications* 31: e02383.

U.S Army Corps of Engineers. 2023. "Combined Operational Plan (COP) 2023 Biennial Report." <https://www.saj.usace.army.mil/Missions/Environmental/Ecosystem-Restoration/G-3273-and-S-356-Pump-Station-Field-Test/>.

U.S. Geological Survey. 2019. "The National Map – Data Delivery." <https://www.usgs.gov/the-national-map-data-delivery>.

U.S. Geological Survey. 2020. "Everglades Depth Estimation Network (EDEN)." <https://sofia.usgs.gov/eden/>.

United States v. SFWMD, et al. 1988. *Case No. 88-1886-CIV-MORENO—Settlement Agreement*. Miami, FL: United States District Court Southern District of Florida, Miami Division.

Van der Valk, A. G., and B. G. Warner. 2008. "The Development of Patterned Mosaic Landscapes: An Overview." *Plant Ecology* 200: 1–7.

Vermeer, J. G., and F. Berendse. 1983. "The Relationship between Nutrient Availability, Shoot Biomass and Species Richness in Grassland and Wetland Communities." *Vegetatio* 53: 121–26.

Williams-Jara, G. M., A. Espinoza-Tenorio, C. Monzón-Alvarado, G. Posada-Vanegas, and D. Infante-Mata. 2022. "Fires in Coastal Wetlands: A Review of Research Trends and Management Opportunities." *Wetlands* 42: 56.

Wu, Y., K. Rutchey, S. Newman, S. Miao, N. Wang, F. H. Sklar, and W. H. Orem. 2012. "Impacts of Fire and Phosphorus on Sawgrass and Cattails in an Altered Landscape of the Florida Everglades." *Ecological Processes* 1: 8.

Yu, L., Y. Huang, F. Sun, and W. Sun. 2017. "A Synthesis of Soil Carbon and Nitrogen Recovery after Wetland Restoration and Creation in the United States." *Scientific Reports* 7: 7966.

Zedler, J. B. 2000. "Progress in Wetland Restoration Ecology." *Trends in Ecology & Evolution* 15: 402–7.

Zedler, J. B., and S. Kercher. 2005. "Wetland Resources: Status, Trends, Ecosystem Services, and Restorability." *Annual Review of Environment and Resources* 30: 39–74.

Zhao, Q., J. Bai, L. Huang, B. Gu, Q. Lu, and Z. Gao. 2016. "A Review of Methodologies and Success Indicators for Coastal Wetland Restoration." *Ecological Indicators* 60: 442–452.

Zweig, C. L., and W. M. Kitchens. 2008. "Effects of Landscape Gradients on Wetland Vegetation Communities: Information for Large-Scale Restoration." *Wetlands* 28: 1086–96.

Zweig, C. L., and W. M. Kitchens. 2009. "Multi-State Succession in Wetlands: A Novel Use of State and Transition Models." *Ecology* 90: 1900–1909.

SUPPORTING INFORMATION

Additional supporting information can be found online in the Supporting Information section at the end of this article.

How to cite this article: Nocentini, Andrea, Jed Redwine, Evelyn Gaiser, Troy Hill, Sophia Hoffman, John S. Kominoski, Jay Sah, Dilip Shinde, and Donatto Surratt. 2024. "Rehydration of Degraded Wetlands: Understanding Drivers of Vegetation Community Trajectories." *Ecosphere* 15(4): e4813. <https://doi.org/10.1002/ecs2.4813>